AALTO UNIVERSITY SCHOOL OF ELECTRICAL ENGINEERING
Department of Radio Science and Engineering

Jukka-Pekka Göran Porko

Radio frequency interference in radio astronomy

Master's Thesis submitted in partial fulfillment of the requirements for the degree of Master of Science in Technology.

Espoo, May 11, 2011

Supervisor: Professor Martti Hallikainen

Instructor: Petri Kirves, M.Sc.

AALTO UNIVERSITY SCHOOL OF ELECTRICAL ENGINEERING

ABSTRACT OF THE MASTER'S THESIS

Author:	Jukka-Pekka Göran Porko	
Name of the Thesis:	Radio frequency interference in radio astronomy	
Date:	May 11, 2011	**Number of pages:** 77
Department:	Department of Radio Science and Engineering	
Professorship:	Space Technology	**Code:** S-92
Supervisor:	Prof. Martti Hallikainen	
Instructor:	Petri Kirves, M.Sc.	

Radio astronomy is a subfield of astronomy, which studies celestial objects with highly sensitive radio receivers and large radio telescopes. These radio astronomical measurements are performed in a wide range of frequencies which are limited by the radio window set by the attenuation in the Earth's atmosphere and the man-made radio frequency interferences (RFI). This thesis discusses, measures and identifies these man-made RFIs, their effect on these sensitive measurements and the methods to mitigate their effects on the observation.

The external radio frequency environment in the Metsähovi Radio Observatory was measured in the summer of 2010 with an antenna and a spectrum analyser in several frequency bands. As radio astronomical measurements are also vulnerable to the self-generated RFIs of the observatory, a few corresponding measurements were performed to determine the state of the internal radiation. Three radio receivers were tested to estimate the impact of external and internal RFIs on radio astronomical measurements. To identify the interference sources and their origin, a spectrum analyser was connected to the intermediate frequency (IF) port of a radio receiver, while the radio telescope was set to sweep the horizon with a low elevation.

The most significant external RFI sources discovered in this study consisted of Digital Video Broadcasts (DVB), GSM, UMTS (3G-network), aviation radio broadcasts and radio amateur activity. The strongest detected internal interference sources comprised cell phones and microwave ovens. This thesis also proposes a new radio frequency interference monitoring equipment to guarantee the safety of the radio astronomical observation in Metsähovi in the future.

Keywords: radio astronomy, RFI, Metsähovi

AALTO YLIOPISTON
SÄHKÖTEKNIIKAN KORKEAKOULU

DIPLOMITYÖN TIIVISTELMÄ

Tekijä:	Jukka-Pekka Göran Porko	
Työn nimi:	Radio frequency interference in radio astronomy	
Päivämäärä:	11.5.2015	**Sivuja:** 77
	Radiotieteen- ja tekniikan laitos	
Professuuri:	Avaruustekniikka	**Koodi:** S-92
Työn valvoja:	Prof. Martti Hallikainen	
Työn ohjaaja:	DI Petri Kirves	

Radioastronomissa mitataan heikkojen taivaallisten kohteiden säteilyä lähes koko ilmakehän suomassa taajuusikkussa. Mitattava säteily on luoteeltaan heikkoa kohinaa, jonka mittaamiseen tarvitaan herkkiä radiovastaanottimia. Radioastronomisia mittauksia rajoittavat ilmakehän vaimennuksen lisäksi merkittävästi myös ihmisten tuottamat radiohäiriöt. Tämän diplotyön tarkoituksena on selvittää mitä nämä ihmisten aiheuttamien radiohairiöt ovat, miten ne vaikuttavat radioastronomisiin mittauksiin ja mitä niiden vaikutusten minimoimiselle on tehtävissä.

Radiohäiriö mittaukset suoritettiin Metsähovin radio observatoriossa kesällä 2010 usealla eri taajuuskaistalla. Näiden radiohäiriöiden mittaamiseen käytettiin spektrianalysaattoria ja parabolista antennia. Ulkoisten radiohairioiden lisäksi diplomityössä tutkittiin myös observatorion itsessään synnyttämää häiriösäteilyä. Radioympäristön vaikutusta radiovastaanottimien toimintaan tutkittiin usealla eri vastaanottimella, nauhoittamalla spektrianalysaattorilla radiovastaanottimen välitaajuuskaistan spektriä, kun radioteleskoopi asetettiin keilaamaan horisonttia matalalla elevaatiolla.

Radioympäristön mittauksissa voimakkaimmiksi häiriötekijöiksi osoittautuivat digitaaliset televesiolähetykset, matkapuhelin taajuudet, ilmailun radioliikenne ja navigointi ja radioamatöörilähetykset. Observatorion sisäisistä häiriöstä voimakkaimmat olivat peräsin mikroaaltouunista ja matkapuhelimista. Jotta myös tulevaisuudessa voidaan radioastronomisten mittausten luotettavuus taata jatkuvasti kasvavassa häiriöympäristössä, esitellään myös suunnittelu ehdotus uudesta radiohäiriömonitorista.

Avainsanat: radioastronomia, radiohäiriö, Metsähovi

Acknowledgements

I would like to thank Professor Merja Tornikoski for granting me this opportunity to do my master's thesis on a fascinating topic at the Metsähovi Radio Observatory. I also like to express my appreciation to Professor Martti Hallikainen for his time, patience and guidance. Special thanks to my instructor Petri Kirves, for helping me in planning and executing my measurements, without his efforts this thesis would not exist in it's present form. Also special thanks to Juha Kallunki for his time and assistance and for providing me all the tools to carry out my measurements. Erkki Oinaskallio, Jouko Ritakari and Miika Oksman, I really appreciate your advices and assistance. Special thanks go to the rest of the Metsähovi staff for their pleasant company and the positive working atmosphere.

Otaniemi, May 11, 2011

Jukka-Pekka Göran Porko

Contents

Symbols and Abbreviations

Symbols

α	False alarm rate
ϵ	Antenna efficiency
Γ	Gamma function
λ	Wavelength
$\mu_{\chi^2(v)}$	Mean value estimate
ρ	Polarization mismatch
τ	Integration time
θ	Angular resolution
AF	Antenna factor
A_P	Physical aperture
B	Bandwidth
B_n	Noise bandwidth
c	Speed of light 299 792 458 [m/s]
d	Diameter
D	Directivity of an antenna
e	Elevation
e_A	Aperture efficiency

f	Frequency
Δf	Frequency bandwidth
F_n	Noise figure
F_{RFI}	RFI flux density
G	Gain
h	Planck's constant 6,620$\times 10^{-34}$ [Js]
k	Boltzmann's constant 1,380$\times 10^{-23}$ [JK^{-1}]
L	Attenuation
m_n	Moment
M	Number of samples
N_{SYS}	System noise power
P	Power
RB	Resolution bandwidth
R	Kurtosis value
S	Power spectral density
T_A	Antenna temperature
T_{cold}	Cold load temperature
T_{hot}	Hot load temperature
T_r	Receiver noise temperature
ΔT_{min}	Sensitivity
Y	Y-term

Abbreviations

AOS	Acousto Optical Spectrometer
BPF	Band Pass Filter

DME	Distance Measurin Equipment
DOA	Direction-of-arrival
DSB	Dual Side Band
FICORA	Finnish Communications Regulatory Authority
GPR	Ground Penetrating Radar
GPRS	General Packet Radio Service
GSM	Group Special Mobile
HPBW	Half Power Beam Width
HVAC	Heating, Ventilation, Air Conditioning
IF	Intermediate Frequency
LNA	Low Noise Amplifier
LO	Local Oscillator
NMT	Nordic Mobile Telephone
RFI	Radio Frequency Interference
SIS	Superconductor-Insulator-Superconductor
SK	Spectral Kurtosis
SOI	Signal-of-interest
spfd	Spectral Power Flux Density
SSB	Single Side Band
SSR	Short Range Radar
STUK	Finnish Radiation Safety Centre
VLBI	Very Large Baseline Interferometry
WPR	Wall Penetrating Radar

Chapter 1

Introduction

1.1 General

In radio astronomy, astronomers use highly sensitive radio receivers to detect and study weak celestial radio emissions. Almost the whole radio frequency spectrum contains valuable information of the physical nature of the universe. In ground-based radio astronomy, this frequency spectrum is limited by the attenuation of the Earth's atmosphere and the man-made radio frequency interferences (RFI). The Earth's atmosphere is transparent to electromagnetic radiation from 30 MHz to 300 GHz; within this radio window the biggest spectrum limiting factor in radio astronomical studies are the man-made RFI. These radio interferences are often much stronger than the weak noise type celestial radio emissions, and therefore may cause serious distortion to the data.

All the radio observatories throughout the world have to coexist with surrounding interfering radio environment. The growing number of different types of radio applications and gadgets are deteriorating the radio frequency spectrum each year. Consequently radio observatories are obligated to monitor the ambient radio environment constantly to ensure the safety of the astronomical measurements. Radio observatories themselves are also a significant source of harmful radiation, which needs to be monitored as well. Due to the sensitive nature of radio astronomical measurements, observation is often performed in a protected frequency band reserved for radio astronomical use only.

The Metsähovi radio observatory (MRO) is located 45 km due west from Helsinki city center. All the radio receivers employed in Metsähovi are operating in protected

frequency bands between 22-175 GHz. Since these radio receivers are operating in such high frequencies, a down conversion of the RF signal is mandatory. These down converted intermediate frequencies (IF) vary, depending on the receiver, between 0.2-1.6 GHz. Strong enough RFI might penetrate the shielding of the receiver chain, and interact with the astronomical signal in the IF channel. To ensure the safety of the astronomical measurements, RFIs need to be monitored in the signal band as well as in the down-converted IF band. The surrounding radio frequency environment in the MRO has been monitored since the year 1998 in a 400-2000 MHz frequency band, which unfortunately covers only the IF band of the radio receivers.

1.2 The structure of this thesis

In this thesis, we first introduce a brief literature part concerning radio astronomy in general, the employed observation methods and the structure of a radio receiver and a radio telescope. We present the harmful internal and external RFI sources and discuss their possible impact on the astronomical measurements. Multiple mitigation methods are also introduced to deal with these harmful interferences. RFI data has been collected in Metsähovi since 1998, the evolution of the ambient radio environment is also discussed in the thesis. A new steerable RFI monitor was built in the observatory grounds in the summer 2010. With the help of this new equipment, more wideband and directional information was gathered from the surrounding radio environment. This RFI data was collected with horizontal and vertical polarization between 350-2600 MHz. Radio observatories are also suffering from their self-generated radio interferences, therefore the internal radiation was measured as well in the 30 - 2600 MHz frequency band. To improve the RFI detection in the future in Metsähovi, a new RFI-monitoring system is also introduced in the thesis.

Determining the effects of the RFIs in the radio astronomical observation, three radio receivers were tested in their normal observational situation. The radio telescope was set to sweep the horizon with low elevation, meanwhile the IF channel of the receiver was measured with a spectrum analyser. Some of these tested receivers were clearly suffering from the presence of the RFI, even though they are operating at protected frequency bands reserved for astronomical use only.

Chapter 2

Introduction to radio astronomy

2.1 The discovery of radio astronomy

Radio astronomy is a relatively new form of astronomy, which was first discovered in the 1930s by a radio engineer named Karl Jansky. He was studying short wave radio frequency interferences in the transatlantic radio telephone services in the Bell Telephone Laboratories. His assignment was to determine the source of the unknown static in radio voice transmissions. Jansky built a rotating antenna system for his measurements operating at 20.5 MHz, shown in Figure 2.1. In his studies, Jansky found three different types of interferences. He inferred that two of these interferences were caused by nearby and more distant thunderstorms, but the origin of the third weak noise like interference remained unknown for a while. It took him several months to identify the source of this third unknown static. He realized that the interference had to have an extraterrestrial origin. His first guess was the Sun, but as he continued his measurements Jansky noticed that the strongest radiation was coming from the center of the Milky Way. Jansky published his measurements in December 1932, after over one year of observation. Soon after publishing his paper Jansky was reassigned to other duties, because the interfering radiation from the Milky Way was the least of the problems in the transatlantic radio telephone transmissions. The second pioneer in radio astronomy was Grote Reber, who was the first to understand the significance of Jansky's findings. He continued Jansky's work by building a 9.5 meter parabolic radio telescope in his own backyard in Wheaton, Illinois. Reber also wanted to work in a wider range of frequencies than Jansky. He built several radio receivers but, unfortunately, many of them failed to detect extraterrestrial radiation. His third receiver, operating at 160 MHz was successful and he was finally able to verify Jansky's results.

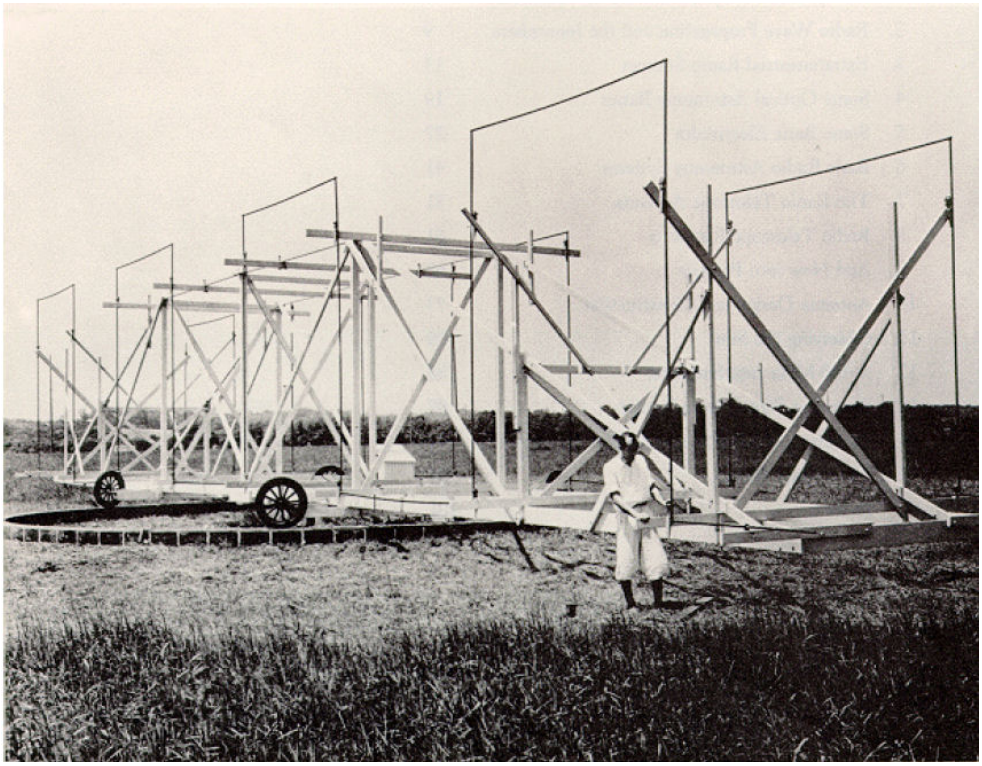

Figure 2.1: Karl Jansky's rotating antenna system operating at 20.5 MHz. [1]

Even in the late 1930s Grote Reber had to deal with man-made RFIs like the radio astronomers today. He lived in a suburban area of Chicago, where he was obligated to work only during the night-time due to the harmful radiation from automobile engines. Reber continued his measurements for many years to complete the first map of the radio sky, which he published in 1944. At first the astronomical society was sceptic of his results, but soon after the Second World War more and more research groups around the globe started building bigger and better antennas and receivers to continue Jansky's and Reber's groundbreaking work. At this point radio astronomy started growing by leaps and many remarkable discoveries were made; some of them even received a Nobel Prize.

In 1951 the HI emission line (21.1 cm) was discovered, which led to the study of the dynamics and composition of our own Galaxy in radio astronomy. The interest towards radio astronomy increased even more rapidly during the 1960s. The most important discoveries of that era were the quasars, the 3 Kelvin background radiation and the pulsars.[1]

2.2 Modern radio astronomy

The scientific instruments applied in radio astronomy have evolved remarkably since the early days of Jansky and Reber. Radio astronomical studies are now done in a much wider frequency range, from 30 MHz to 300 GHz. Modern technology has made it possible to build more and more sensitive radio receivers for astronomical studies, to see beyond our own Galaxy to the far edge of the whole universe. To gather more radiation from the distant celestial radio sources, the size of the radio telescopes has increased significantly. The world's biggest non steerable radio telescope in Arecibo Puerto Rico is 305 meters in diameter. The largest fully steerable radio telescope is 100 meters in diameter, it is located in Green Bank, West Virginia. [2, pp.245-248]

2.2.1 Radio astronomical telescopes

The most popular antenna type in radio astronomy is the Cassegrain telescope, like the one in the Metsähovi radio observatory, shown in Figure 2.2. This telescope type consists of a parabolic primary reflector, a secondary hyperbolic reflector and the feed antenna which is located in the focal point of the hyperboloid. The secondary reflector is located in the central axis of the primary reflector to reflect all the incoming plane waves into the antenna feed.

The most critical parameters in parabolic antenna dish design are the antenna gain, surface accuracy and the half power beam width (HPBW). The antenna gain is defined by the surface area A of the dish and the operating frequency f or the wavelength λ, see Equation (2.1).[3, Chapter 3, pp.7-11]

$$G_A = \frac{4\pi}{\lambda^2}\eta_A A_P, \tag{2.1}$$

where e_A is the aperture efficiency and A_P is the physical aperture area of the dish. Since the antenna gain is depending on the wavelength and the surface area of the reflector, low frequency measurements require enormous reflectors to achieve a reasonable angular resolution. HPBW of the parabolic antenna is defined by Equation (2.2), where d is the diameter of the dish and k is a factor depending on the shape of the reflector, which is $\sim$70 for parabolic reflectors.[4]

$$\theta = \frac{k\lambda}{d} \tag{2.2}$$

Figure 2.2: 14 m Cassegrain telescope in Metsähovi Radio Observatory.

The demands for the surface accuracy of the reflector get higher with frequency, which is considered to be greater than $\lambda/10$. Poor surface accuracy will diminish the antenna gain and lead to the increase of the HPBW.[2, pp.245-248]

2.2.2 Radio astronomical receivers

The frequency range used in radio astronomical measurements is often quite high, which makes the down-conversion of the RF signal to IF obligatory. Figure 2.3 illustrates the general structure of a total-power superheterodyne receiver used in high frequency measurements. The incoming celestial radiation is conducted from the antenna feed to the front-end Low Noise Amplifier (LNA) via a waveguide or a coax cable, where the signal goes through the fist stage of amplification. In some receivers the RF signal is also filtered with a Band Bass Filter (BPF) before the down-conversion to IF. The down-conversion of the RF signal f_{RF} is done with a mixer and a Local Oscillator (LO)operating in f_{LO}, giving the output IF signal $f_{IF} = f_{RF} - f_{LO}$ [2].

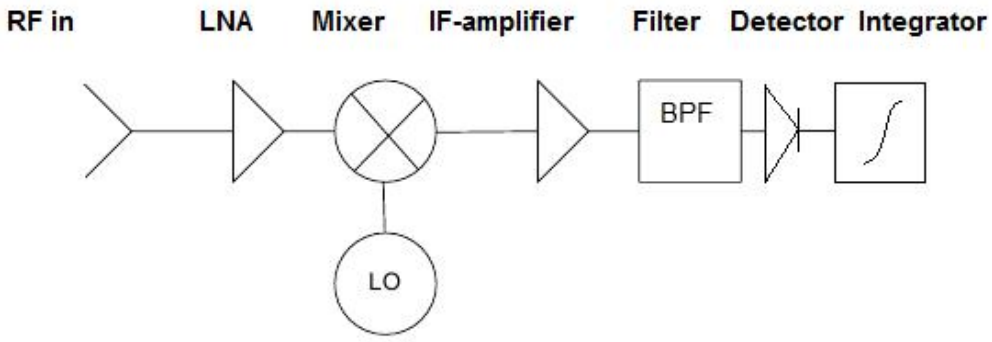

Figure 2.3: The general structure of a total-power superheterodyne receiver.

The Mixer is often a Shcottky-diode or a superconductor-insulator-superconductor (SIS) component. After the down-conversion, starts the IF part of the receiver, where the IF signal is amplified a second time and filtered before the detection. The utilized detector is often a square-law-detector, which converts the altering IF signal to corresponding DC level to make further data processing possible. The DC output signal is integrated in an integrator for several seconds, where the maximum integration time is set by the amplifier stability and the Earth's rotation.[5, pp. 40-47], [6]

Radio receivers are themselves a strong source of noise and therefore their effect in the observation needs to be cancelled out. The detected signal is a combination of the antenna temperature T_A and the receiver temperature T_r, see Equation (2.3) [6]

$$P = kB(T_A + T_r), \tag{2.3}$$

where k is the Boltzmann's constant and B is the observation bandwidth. The sensitivity of the receiver, using an ideal integrator is given by Equation (2.4), where B is low frequency noise bandwidth and τ is the integration time. [6]

$$\Delta T_{min} = \frac{T_A + T_r}{\sqrt{B\tau}} \tag{2.4}$$

Radio receivers are calibrated before the observation session, by measuring the level of self generated noise of the receiver T_r, which will be reduced later in the signal processing. The calibration needs to be done carefully, if the T_r is overestimated it will deteriorate the threshold value which weakens the sensitivity performance of

the receiver. If the T_r is underestimated, the following measurements are distorted by the receiver's own noise power. The receivers self-generated noise can increase when its components get older, therefore continuous calibration is mandatory. The most practical way to calibrate a radio receiver is with the Y-term method, where the noise figure of the receiver is determined with the help of two know noise sources T_{hot} and T_{cold}. The upside of this particular method is that the gain and the noise bandwidth of the receiver do not need to be known. The Y-term is determined as follows, see equation (2.5) [3],

$$Y = \frac{P_{hot}}{P_{cold}} = \frac{(T_r + T_{hot})kGB}{(T_r + T_{cold})kGB} = \frac{T_r + T_{hot}}{T_r + T_{cold}}, \tag{2.5}$$

where G is the receiver gain and k is the Boltzmann's constant. The receiver temperature T_r can be derived from the previous Equation (2.5) [3],

$$T_r = \frac{T_{hot} - YT_{cold}}{Y - 1}. \tag{2.6}$$

The corresponding noise figure F_N to T_r is the amount of noise which needs to be cancelled from measurements, which can be calculated by the Equation (2.7) [3],

$$F_N = 10log(\frac{\frac{T_{hot}}{T_0} - 1}{Y - 1}). \tag{2.7}$$

2.3 Observation methods

Radio astronomical observation methods can be divided into four different groups, continuum, spectral line, solar and interferometric observation. The first three of the methods can be used with a single dish antenna, whereas the last requires a telescope array. All of these observation methods are introduced in this chapter briefly.

2.3.1 Continuum observation

Continuum observation is a study of the long-term variability of celestial objects, such as, Quasars, Active Galactic Nuclei, Pulsars and Supernova remnants. The observed emission from these celestial radio sources are extremely weak, and therefore they produce very little variation into the antenna temperature T_A. The radio receivers applied in the continuum observation use long integration times τ and broad observation bandwidths B to enhance the sensitivity of the receiver, see Equation

(2.4). Long integration time also sets a high stability demand to the receiver's amplifier, in some measurements the amplifier need to be stable for almost 2000 seconds. Continuum observation is vulnerable for man-made radio frequency interference, since the interference is added to the system 100 % coherently.

2.3.2 Spectral line observation

In Spectral line observation, highly sensitive radio receivers are used for studying the content of the interstellar medium. The first and most studied spectral line in radio astronomy is the HI-line, it comes from neutral hydrogen, which can be detected in 1,420 GHz. Now, over a hundred spectral lines have been studied to assess the abundance of different molecules and the dynamics of our galaxy. The velocity and the heading of the interstellar material can be calculated from the Doppler shift of the spectral line. A list of important spectral line frequencies in radio astronomy can be found in [7]. Acousto-optical spectrometers (AOS) are often used as radio receiver instead of the traditional square-law detector in spectral line observation. To enhance the sensitivity of this narrow band observation, long integration times are used, which are limited by the Doppler effect caused by the Earth's rotation. Spectral line observation is extremely vulnerable to RFI, which makes the observation difficult outside the protected frequency bands reserved for astronomical use only.

2.3.3 Solar observation

The Sun is a powerful radiator in the whole frequency spectrum from radio waves to X-ray. Solar observation in radio astronomy includes tracking and mapping of all kinds of radio activities in the Sun. The most studied phenomenons are the radio bursts, gradual bursts, the solar S-component, the 160 min oscillation and coronal mass ejections. Since the Sun is such a powerful radiator, the radio receiver does not need much amplification nor long integration times. This broadband observation is only limited by man-made RFI.

2.3.4 Interferometry

In radio interferometry, higher angular resolution in the radio imaging is achieved with multiple radio telescopes monitoring the same celestial object simultaneously. The distances between the radio telescopes can be enormous, for example in Very Large Baseline Interferometry (VLBI) the telescopes can be located in different continents. The data collected from the different telescopes is combined and correlated

in a central station, where all the geometrical delays and timing errors between the observatories are corrected by synchronizing the data. The high angular resolution is not the only upside of the radio interferometry, observation methods like VLBI are also very tolerant toward RFI, since these effects will be cancelled out naturally in the correlator, due to unique radio environment in each observatory.

2.4 Metsähovi Radio Observatory MRO

The Metsähovi Radio Observatory of the Helsinki University of Technology is located 45 km due west from Helsinki in Kirkkonummi in Kylmälä village. The observatory has been operational since the year 1974. The scientific activities in Metsähovi have continuously involved research in radio astronomy, development of radio astronomical instruments and methods, space research, education and radio frequency interference studies. The research in Metsähovi has been conducted with many different techniques, frequencies and equipment. The studies are mainly concentrated on millimetre and microwave frequencies 100MHz - 150GHz. The employed observation methods are continuum, spectral line and VLBI. Research has also been done in the development of microwave receivers, receiving methods, data acquisition and processing, and antenna technology. The 14.5 meter Cassegrain radio telescope in Metsähovi is depicted in Figure 2.2. Table 2.1 lists all the employed receivers and their characteristics.

Table 2.1: Radio astronomical receivers in the Metsähovi Radio Observatory.

Receiver	Signal Frequency [GHz]	IF-frequency [GHz]	Polarization	Noise Temp. T_r [K]
22 GHz Continuum	21.0-22.0, 22.4-23.4	0.2-1.2	Linear	270
22 GHz VLBI	21.980-22.480	0.5-1.0	LCP / RCP	60
37 GHz Continuum/Solar	35.3-36.3, 37.3-38.3	0.5-1.5	Linear	280
37 GHz Solar	37.0	0.25-1.0	4 Stokes	420
80-115 GHz Spectral Line	80-115	1.0-1.6	Linear	150
(90 GHz) 150 GHz VLBI	(84-115), 129-175	3.7-4.2, 0.5-1.0	LCP / RCP	
new 3 mm VLBI	84-89		LCP /RCP	
Geo-VLBI	8.15-8.65, 2.21-2.35	0.5-0.98, 0.68-0.82	RCP	94, 102
Callisto	0.170-0.780		Horizontal	
RFI-monitor	0.4-2.0		Vertical	

LCP = Left hand Circular Polarization, RCP = Right hand Circular Polarization.

Chapter 3

Radio Frequency Interference

The radio frequency spectrum in ground-based radio astronomy is limited by attenuation in the Earth's atmosphere. The atmosphere is opaque for radio waves below 30 MHz due to the amount of free electrons in the ionosphere, which reflect the radio waves back to the space. The upper limit in the ground-based observation, is set by gas molecules causing attenuation, which becomes significant above 300 GHz. The thus limited part of the radio frequency spectrum is called the radio window. A second spectrum-limiting factor inside this radio window is the man-made radio frequency interference (RFI). These interferences are normally a billion times stronger than the observed weak celestial radio emissions, whereupon they limit the radio spectrum remarkably. All the wireless radio applications, such as, television- and radio broadcast, radars, communication systems etc. are diminishing the usable part of the frequency spectrum in the radio astronomy. Radio observatories are not only vulnerable to external RFIs, they also suffer from internal radiation as well. The strongest internal RFI sources are the computers and the screens, microwave ovens, electric motors and other scientific instruments. In this chapter we introduce different types of RFI sources, estimate their harm levels and their impacts on the radio astronomical measurements.

3.1 Radio frequency allocation

In Finland, the radio frequency spectrum is controlled by the Finnish Communications Regulatory Authority (FICORA), which is an institution under the Ministry of Transport and Communications. FICORA monitors the use of the radio spectrum and the development of new radio applications. The frequency allocation in Finland is presented in Figure 3.1.

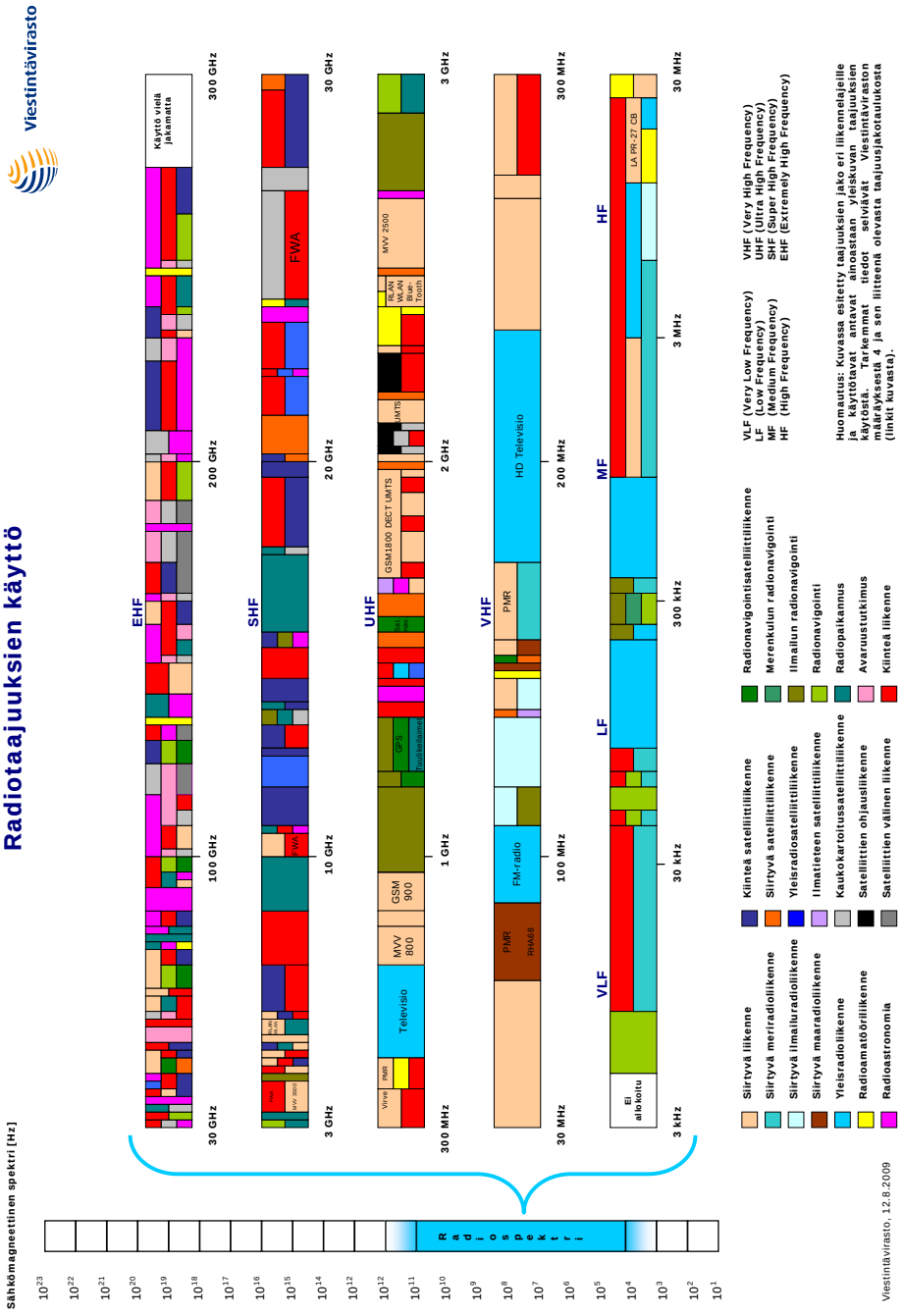

Figure 3.1: Frequency allocation in Finland, Finnish Communications Regulatory Authority (FICORA).

Since radio astronomical observation is so susceptible to man-made RFI, FICORA has arranged several frequency bands reserved for radio astronomical use only. A list of these frequency bands is shown in Appendix A. The protection of these frequency bands is effective around the world to ensure joint observation sessions like VLBI between different countries. International Telecommunication Union (ITU) is the radio frequency spectrum controlling authority worldwide. The fundamentals of the protection criteria for the radio astronomical measurements can be found in ITU's Recommendation ITU-R RA.769-2 "Protection criteria used for radio astronomical measurements".

3.2 Radio frequency interference in radio astronomy

The radio frequency interferences can be divided into two classes, external and internal RFI. External radio interferences come from the surrounding environment from all kinds of radio applications. The radio environment in the radio observatory consist of the constant interferences like the television and radio broadcasts and the transient interferences like radars and aviation radio broadcasts. Constant radio broadcasts are relatively easy to measure and their effects in the astronomical measurements can usually be avoided by choosing an interference free band for the observation. The transient interferences are a little more problematic to detect and their impact on the measurements is difficult to estimate. The elimination of this type RFI requires the use of the complex mitigation methods, which are introduced in Chapter 4.

The observatories are themselves a remarkable source of radio interference. These facilities contain a great number of radiating devices such as computers, scientific instruments, electrical engines, microwave ovens and many others. These internal interferences can be both constant or transient in nature and their influence on the astronomical data can be significant, since these harmful radiators are located so close to the radio telescope and the receiver. In this chapter we present the most common internal and external radio frequency interference sources and estimate their effects on radio astronomical measurements.

3.2.1 External RFI

External RFIs can be divided into two classes, ground based - and aero- and space born RFIs. Ground based RFI is often more harmful due to the high transmission

power and closer localization. Radio astronomical observations are not done with very low elevation, normally never less than 20° due to the high attenuation by the atmosphere. Therefore these RFIs are more likely to contribute to the radio astronomical measurement by leaking in through side lobes of the antenna pattern. Strong enough RFI can also penetrate the shielding of the cable of the receiver and corrupt observed band in the IF channel.

Radio interferences in the observed signal or nearby bands are the most problematic ones, because they will pass through the bandpass filters of the receivers. Most radio astronomical measurements are done in high frequencies in protected frequency bands, where the signal band is not threatened by man-made RFIs. To ensure the safety of the astronomical measurements, the radio frequency spectrum ought to be monitored in the receivers signal (RF) and the down-converted IF band. A list of these ground based RFIs are listed Table 3.1 in 30-3400 MHz band.

Air- and space borne radio interferences are ever increasing due to the growing number of air traffic and satellite telecommunication applications. Air traffic has occupied many frequency bands for radio navigation and communication, Distance Measuring Equipment (DME) and radars. These interferences can be extremely harmful for the observatories located in the active air traffic areas like most of Central Europe. The biggest satellite telecommunications services, such as the Global Positioning System (GPS), GLObalnaja NAvigatsionnaja Sputnikovaja Sistema (GLONASS), Global star and Iridium are providing their services in the whole world from television broadcast to satellite phones services. These space borne RFIs are causing both transient and constant interference to radio astronomical measurement, by leaking in through the main and the side lobes of the antenna pattern. Due to the low transmission powers and the source distance of the space borne RFIs, they are not likely to corrupt measurements in the IF channel. Table 3.1 includes also all the reserved bands for the air- and space borne radio traffic. More precise frequency allocation can be found in FICORA's official web page www.ficora.fi.

Table 3.1: Frequency allocation in Finland for 30-3400 MHz.

Frequency [MHz]	Source
30 - 50	Military applications
50 - 87,5	Military applications Radio amateurs Radio navigation Radio links
87,5 - 108	radio broadcasts
108 - 174	Aviation radio/navigation Military applications Radio amateurs Coastal radio stations
174 - 240	Digital Video Broadcasting (DVB)
240 - 339	Military applications Radio navigation
339 - 400	Radio links State Security Network (VIRVE) TErrestrial Trunked RAdio (TETRA)
400 - 470	Military applications Radio links TErrestrial Trunked RAdio TETRA Radio amateurs Digital wideband broadcasts 450
470 - 790	Digital Video Broadcasting (DVB)
790 - 1000	Military Digital wideband broadcasts 800 Groupe Spéciale Mobile (GSM-900) Aviation radio/navigation Distance Measuring Equipment (DME)
1000 - 1400	Distance Measuring Equipment (DME) Radio navigation Radars Radio amateurs Military
1400 - 1525	Military Radio links Digital Audio Broadcasting (DAB)
1525 - 1710	Satellite telecommunication and navigation
1710 - 2170	Groupe Spécial Mobile (GSM-1800), International Mobile Telecommucations(IMT) Digital wideband broadcasts 2000 Radio links Satellite telecommunication 3G-network (IMT)
2170 - 3400	Satellite telecommunication Radio links Radio amateurs Digital wideband broadcasts 2500 Radio navigation Military Radars

3.2.2 Internal RFI

Radio observatories are themselves a significant source of RFI. Most of these interference causing devices are obligatory for the radio astronomical studies and therefore their use cannot simply be banned. However, there exist multiple ways, which observatories can use to diminish their effects on radio astronomical measurements. It is crucial that these radiating equipments are identified and isolated from the receiving antenna and the receiver. Unfortunately this is not always possible due to practical and economic reasons. Table 3.2 lists the most common internal RFI sources. Their impact on astronomical observation depends greatly on the infrastructural design of the observatory and the shielding of the equipment. All these individual radiating devices together nevertheless raise background noise at observatory site, which will have indefinite impact on the astronomical measurements.

Obligatory scientific instruments, like hydrogen masers are wideband radiators between 1-7 GHz [8], and they ought to be placed inside of a shielded room (Faraday cage). The use of wireless applications, such as bluetooth ought to be prohibited, since they are using 2.4 GHz for data transfer with relatively high power levels 1-100 mW [9]. The telescope steering servo electronics is mandatory for radio telescope steering, unfortunately it's also a source of wideband interference, which needs to be shielded properly [8]. The use of fluorescent lamps and poor quality led lamps ought to be avoided, due to their wideband radiation. Computing equipments like personal computers and notebooks, contain multiple small radiating internal structures working as an antenna, from several hundred MHz to a few GHz. External storage devices are connected to the personal computers via cables, which are also known to

Table 3.2: Internal radio interference sources inside some radio observatories. [8],[9],[14].

INFRASTRUCTURAL RFIs	RFI FROM SCIENTIFIC INSTRUMENTS	OTHERS
Computers, Laptops,Screens	Hydrogen Maser	Car engines (not diesel)
Wireless application; Bluetooth, Wireless Local Area Network (WLAN)	Antenna steering servo electronic	Parking radars
Fluorescent lamp	Scientific instruments, signal generator, spectrometers	Microwave ovens
Heating, Ventilation, Air conditioning (HVAC)		Cell phones
Keyboard Video Mouse (KVM) box		
Disk units		

generate abundant levels of radiation, and therefore they should be regarded with suspicion. Computer monitors, CTR and TFT are also a source of relatively high interference, possibly due to poor internal shielding. A radio observatory also contain plenty of mandatory high speed digital measuring equipment leaking wideband radiation. Even the RFI mitigation systems used for removing interferences from the receiver's baseband, generate remarkable amounts of radiation. Poor quality RFI monitoring system may also cause narrow band RFI by radiating the energy back through the antenna connection [9].

3.3 Harmful RFI levels

The presence of RFI, internal or external, can corrupt the radio astronomical observation in many ways. In the worst case, strong enough RFI can saturate the receiver's amplifier response or even break it down. Some GaAs-FET and HEMT amplifiers can break down, when the interfering signal levels are between $\sim$ 0.1 W...0.01 W. The corresponding power flux density if the interference leaks in through the isotropic side lobe is -10 to +40 dBW/m^2,[10, pp.258-266]. Depending on the receivers and the amplifiers within, the estimated values which will inflict one-percent gain compression in the amplifier response are between -70...-30 dBW/m^2 at centimetre wavelengths, when the interference leaks in through the isotropic side lobe [10, pp.258-266]. The sensitivity of the receiver is determined by the system noise temperature, see Equation (2.4). The tolerance towards the RFI ought to be compared to the sensitivity of the receiver, see Equation 3.1. In normal observation, tolerating 10 % of the RFI power level with respect to the system noise is adequate. [11]

$$\frac{N_{RFI}}{N_{SYS}} = \frac{F_{RFI}\frac{\lambda^2}{4\pi}}{kT_{SYS}B}, \tag{3.1}$$

where F_{RFI} is flux density of the RFI. The harmful interference level F_{RFI} in single-dish total power radio telescope, according C.C.I.R. Report 224-6 (1986a), equals one tenth of the r.m.s noise level which sets the thresholds for the data, see Equation (3.2).[10]

$$F_{RFI} = \frac{0.4\pi f^2 k T_{sys}\sqrt{B}}{c^2 G_a \sqrt{\tau}}, \tag{3.2}$$

where B is the observed bandwidth, G_a is the antenna gain and τ is the integration time used for observation. The corresponding equation for the RFI threshold in Very Long Baseline Aperture-synthesis is presented in Equation (3.3).[10]

$$F_{RFI} = \frac{0.4\pi f^2 k T_{sys} B}{c^2 G_a}, \tag{3.3}$$

where c is the speed of light and k the Boltzmann constant. In the VLBI observation, the harmful RFI level is 40 dB greater than in the single-dish observation, since the measurements are based on a correlation [11]. Harmful threshold levels of RFI, for the continuum and the spectral line observation are found in Recommendation ITU-R RA.769-2 Protection criteria for radio astronomical measurements [12], see Table 3.3.

Table 3.3: Harmful interference threshold levels in the continuum (left) and the spectral line (right) observation. In these estimates, the antenna gain is 0 dBi and the integration time is 2000 s.[12],[13]

Continuum observation Frequency [MHz]]	Channel bandwidth Δf [kHz]	Noise temp. T_{sys} [K]	Interference levels S $[dB(Wm^{-2}Hz^{-1})]$	Spectral line observation f_C [MHz]]	Channel bandwidth Δf [kHz]	Noise temp. T_{sys} [K]	Interference levels S $[dB(Wm^{-2}Hz^{-1})]$
325.3	6.6	100	-258	327	10	100	-244
1413.5	27	22	-255	1420	20	22	-239
2695	10	22	-247	1612	20	22	-238
4995	10	22	-241	1665	20	22	-237
10650	100	22	-240	4830	50	22	-230
15375	50	30	-233	14488	150	30	-221
22355	290	65	-231	22200	250	65	-216
43000	1000	90	-227	43000	500	90	-210
89000	8000	42	-228	88600	1000	42	-208

3.4 Effects of the RFI in the observation

The exact effects of the radio interference are often arduous to estimate in the astronomical measurements. In this paragraph we present some examples regarding RFI corrupted measurements and the typical RFI sources in other observatories. The first example in Figure 3.2, presents the amount of domestic interference from a Ethernet switch in S- and CH-band. Figure 3.3 illustrates the distorted IF-channel

spectrum of a S-band receiver in Yebes radio observatory in Spain. The interference source in this case is the servo electronics.

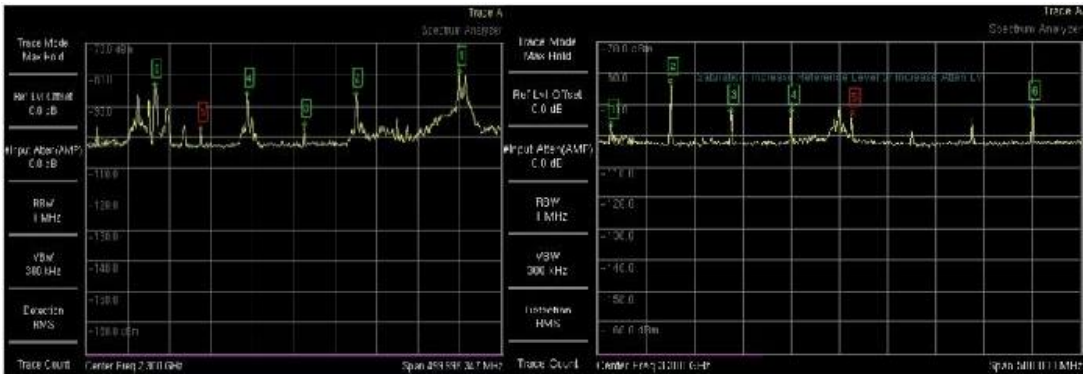

Figure 3.2: Domestic interference from an Ethernet switch, S-band (left) and CH-band (right). [8]

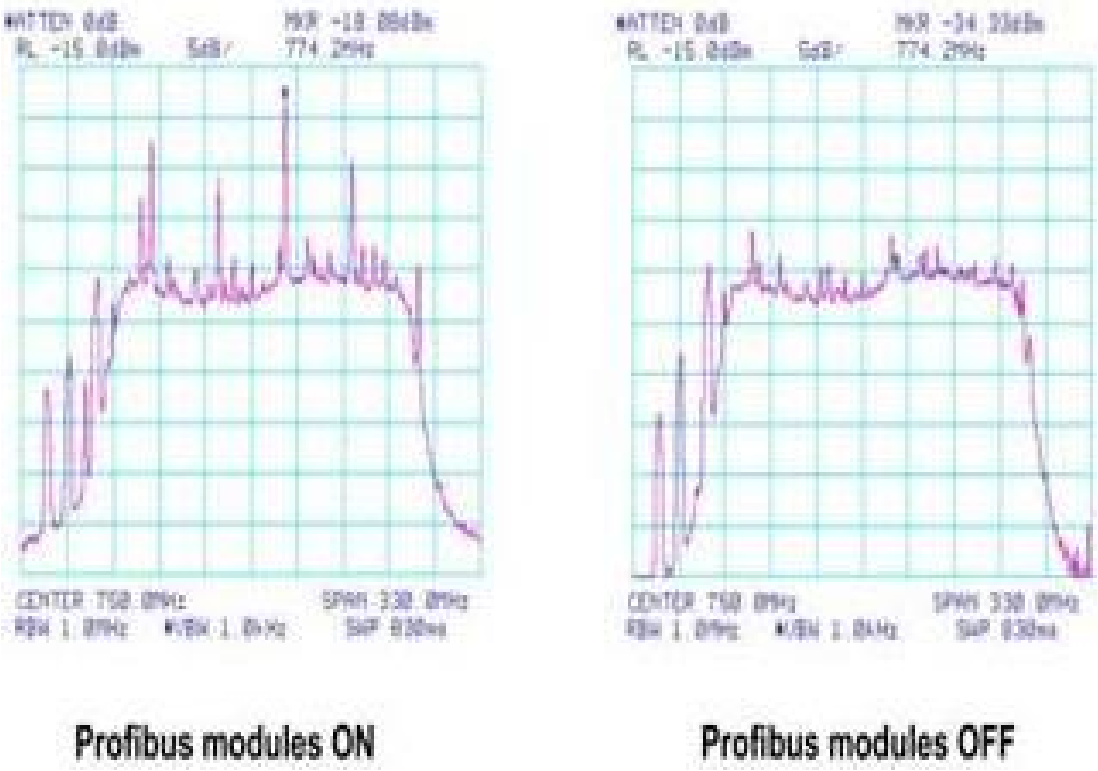

Figure 3.3: Interference from servo electronic in an S-band receiver.[8]

Figures 3.4 and 3.5 present two RFI measurements in Effelsberg radio observatory in Germany. The first plot illustrates the internal RFI around 1620 MHz, the suspected interference source in this case is the PC, media converter or a webcam. In the second plot, the 4.2-4.4 GHz band was recorded during two hours to investigate the amount of interference from airplane radar altimeters.

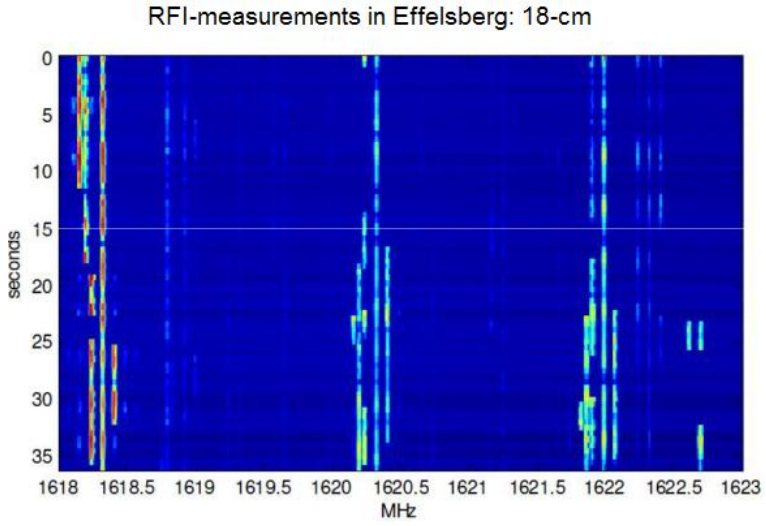

Figure 3.4: Domestic RFI measurement in Effelsberg in 1.6 GHz.[14]

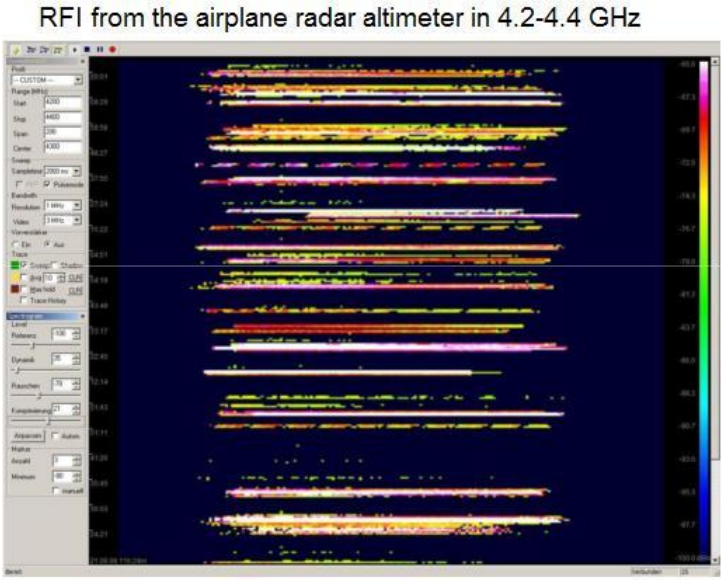

Figure 3.5: RFI from an airplane radar altimeter in 4.2-4.4 GHz in Effelsberg [14]

3.5 RFI monitoring techniques and equipment

Various RFI monitoring systems are used in radio observatories all over the world, to determine the state of the surrounding radio frequency environment. The growing number of radio applications is deteriorating the radio frequency spectrum every year, consequently continuous RFI monitoring is obligatory. The information on the ambient radio environment is often gathered with an antenna measuring vertical or horizontal polarization from several directions. The standard RFI monitoring equipment consist of an antenna, an amplifier and a spectrum analyser. The chosen RFI monitoring frequency band depends greatly on the frequency band used for the astronomical observation. The part of the frequency spectrum where the IF channels of the radio receivers are located, should be investigated as well. These down-converted IF signals are commonly located between 300-3000 MHz.

The RFI antenna or antennas ought to be placed in the same height as the actual radio telescope. Directional information on the RFIs can be gathered in two ways. First, mounting an antenna on a rotating pole, which is set to stop, for example in eight directions to scan the chosen frequency spectrum under interest. The second option is to attach, for example eight antennas on a pole every 45° and to set them to scan the horizon one at a time. Log-periodic antenna, with a 4 to 7 dBi antenna gain is a good low cost choice for this kind of measurement. The sensitivity S (Wm^{-2} $\mathrm{Hz}^{-}1$) of the receiving system is a crucial parameter, which can be determined by Equation (3.4). [13]

$$S = \rho(\varepsilon D)^{-1} \cdot 4\pi f_c^2 c^{-2} \cdot kT_{sys} \cdot (\Delta f \tau)^{-0.5}, \tag{3.4}$$

where ρ is the mismatch between the polarizations, ε is the antenna efficiency, D is the directivity (gain) of the antenna, T_{sys} is the system temperature of the receiving system, Δf is the channel bandwidth and τ is the integration time. The sensitivity can be enhanced with a low-noise-amplifier, where 30 dB gain is often adequate. The ideal RFI-monitoring system sensitivity should match the far-sidelobe sensitivity of a low noise radio telescope [15]. The applied channel bandwidth in RFI-monitoring systems regularly varies between 10-500 kHz. Altogether, the sensitivity of the receiving system ought to be good enough to detect the harmful interference levels determined by ITU-R RA. Rec 769-2. A list of these harmful interference levels for spectral line and continuum observation is found in Table 3.3.

To harvest the RFI data, a computer is connected to the measuring spectrum analyser via Ethernet cable. The collected data is stored into the archive, in a log-file containing 24 hours worth of RFI data. In this way the RFI data can be illustrated with the help of Matlab software, over a chosen period of time. The effects of the transmission path ought to be compensated from data, which can be easily done with Matlab before plotting the RFI data. In Chapter 5 we present the current RFI monitoring system employed in Metsähovi radio observatory. To create some comparison between different RFI monitoring equipments, Figures 3.7 and 3.6 introduce the monitoring system used in Instituto di Radioastronomia in Italy (INAF) and the plotted RFI data between 50-2000 MHz with horizontal H and vertical V polarization.

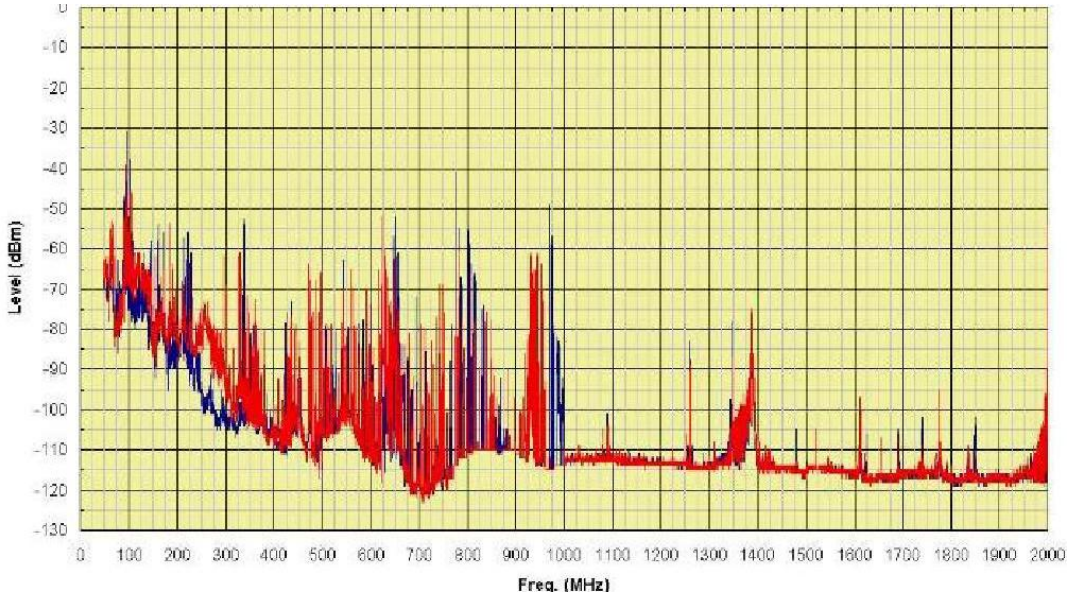

Figure 3.6: RFI data in 50-2000 MHz band, horizontal and vertical polarization (INAF).[11]

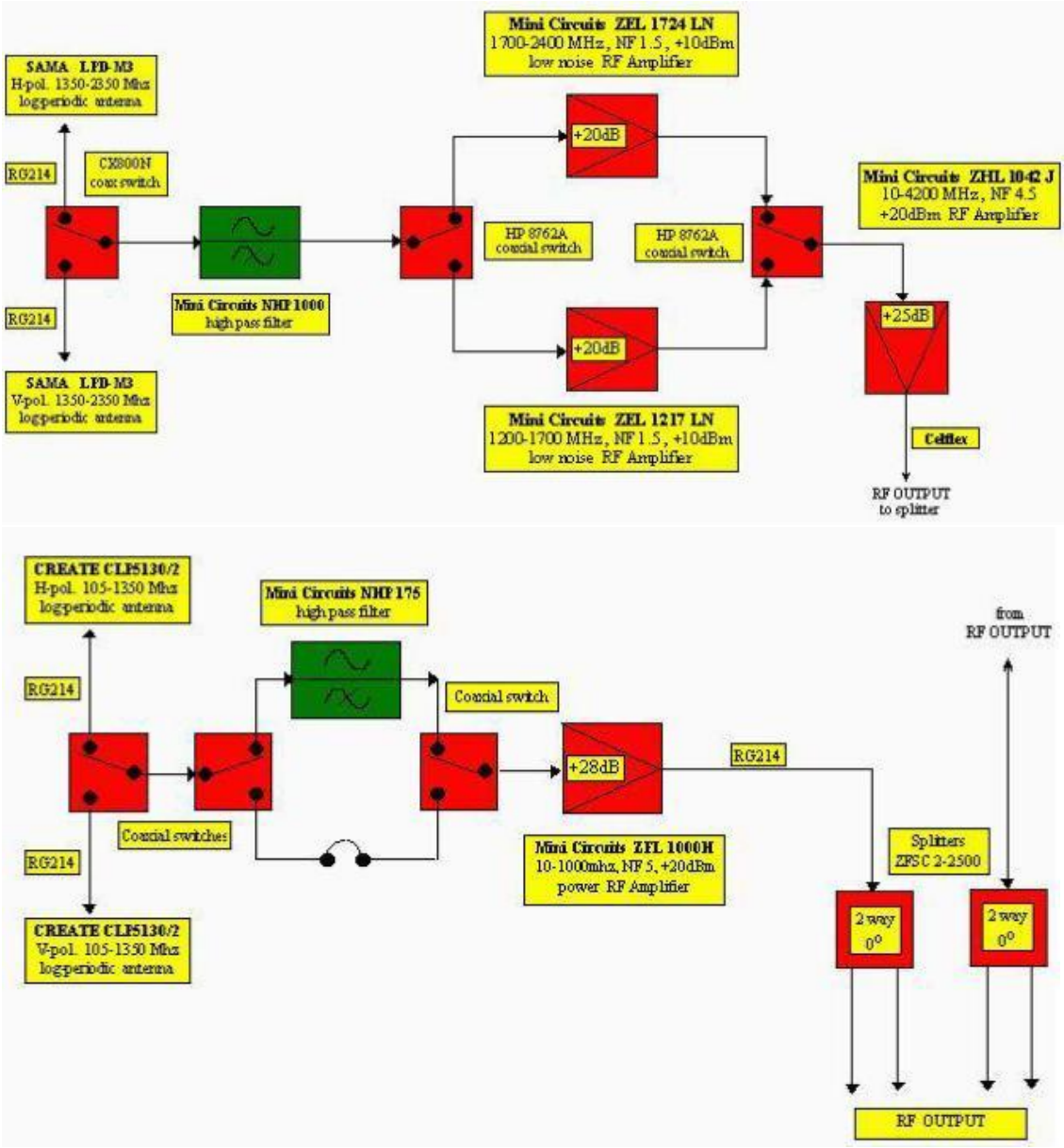

Figure 3.7: RFI-monitoring system employed in INAF. [11]

Chapter 4

RFI mitigation methods in radio astronomy

The increased amount of radio frequency interference has lead to the development of several mitigation and excision methods in radio astronomy. This chapter introduces promising pro- and reactive mitigation methods used in astronomical observation, to coexist with the ambient interfering radio environment.

4.1 Pro-active mitigation strategies

One of the best ways to ensure the safety of radio astronomical measurements is by choosing the protected frequency bands for the measurements, see Appendix A. To avoid high RFI levels, radio observatories are often located in remote or semi-remote areas, where the external interference levels are minimum. In some countries, observatories have been granted special protection by their local licensing authority, to set radio quiet zones around the observatory. These radio quiet zones are usually only one or two kilometres in radius, yet this can be adequate to dampen the nearby interferences under harmful threshold [16]. Radio observatories themselves can contribute to the amount of self-generated RFI via sensible infrastructural design, by shielding all the radiating devices inside a Faraday cage and prohibiting the use of radio transmitters of all kind [9]. Radio receiver design, also plays an essential part in the protection of the astronomical measurements. Receivers are generally placed inside a shielded metal box, which attenuate the RFIs significantly. Inside the receiver, certain radiating analogical electronics are placed inside internal boxes to minimize their impact on the other components. [17]

4.2 Reactive mitigation methods

Some of the observatories are satisfied with their surrounding radio environment and the efficiency of the pro-active mitigation methods. Depending on the nature of radio astronomical studies and the surrounding radio environment, the use of reactive mitigation methods might be mandatory. This chapter introduces few promising mitigation and excision methods in radio astronomy, such as blanking, spatial filtering, adaptive cancellation and digital Kurtosis.

4.2.1 Blanking in time and frequency

Time blanking is an effective and simple mitigation method against transient interferences. To prevent the contamination of the data, a threshold level is established to distinguish the presence of the RFI from the RFI-free state. When the threshold level is exceeded by the attendance of the RFI, the contaminated part of the data will be deleted, see Figure 4.1. The estimate for the threshold level in observation is determined by Equation (4.1), [18]

$$Threshold = 2\frac{\mu_{\chi^2(v)}}{v}P^{-1}(\frac{v}{2}, 1-\alpha), \tag{4.1}$$

where $\mu_{\chi^2(v)}$ is the mean value estimate of the data, α is admissible false alarm rate and P is the normalized Gamma function, see Equation (4.2).[18]

$$P = \frac{\Gamma(v,x)}{\Gamma(v)} = \frac{1}{\Gamma(v)} \cdot \int_0^x t^{v-1}e^{-t}dt, \tag{4.2}$$

The blanking operation can be done with the raw IF channel DC voltages or

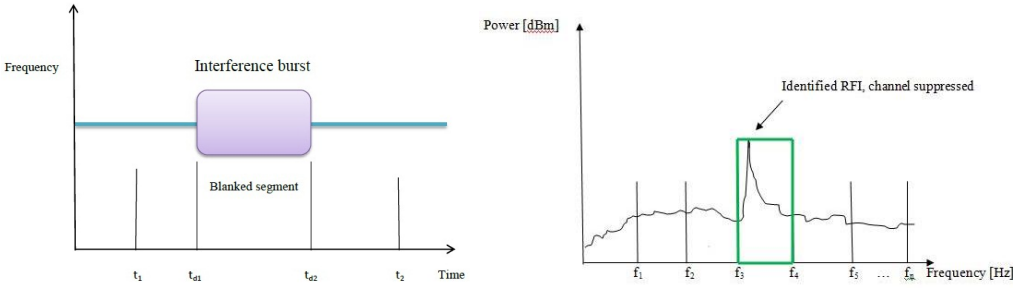

Figure 4.1: In time blanking (left), the segments exceeding the threshold are deleted. In frequency blanking (right), contaminated frequency channels are suppressed.[19],[20]

with the post-detection data. Time blanking is a low cost and easily implemented mitigation method. The downside of this method is that it does not provide any protection against constant broadband RFIs. The only technical demand in this technique comes from the utilised observation bandwidth, which requires the processor to operate on a digitised data stream several hundred MSamples/sec [20]. Unfortunately weak and long lasting radio interferences cannot be recognized in the temporal time domain with the use of a threshold. Rejection of the contaminated data can also be done in the frequency domain, to distinguish RFI from RFI-free spectrum. In frequency blanking, the observation band is divided in multiple equal sized channels Δf, where the RFI contaminated channels are simply suppressed, see Figure 4.1 (right).[21, pp.327-344]

4.2.2 Spatial filtering

Spatial filtering is used in interferometric radio astronomy to remove continuously present RFIs, such as digital video broadcasts, FM-radio broadcasts and GPS signals [22, pp.64-66]. Spatial filtering is based on the difference between direction-of-arrival (DOA) interfering radio broadcast and the direction of the signal-of-interest (SOI). Spatial filtering can also be applied in a single dish observation, by using a low gain auxiliary antenna for the RFI detection [21]. Around the observatory spatially localized RFIs, can be suppressed to minimum by pointing the zeros of the synthesized antenna pattern towards the DOA interference. This type of null-forming is a relatively effective method against RFIs from the telecommunication satellites, e.g. GLONASS and GPS. It is considered to be less effective against ground-based RFI, due to the scattering and the multipath propagation of the interference signals.[23]

4.2.3 Cancellation

Cancellation methods, such as, adaptive and post-correlation are often superior to most excision methods due to the data loss caused by simple blanking. The functioning principles are basically the same in both methods, the harmful RFIs are suppressed to minimum with the help of a reference channel. The weak astronomical signal X_{sig} in the main lobe is often distorted by a presence of a strong interference signal RFI_{main} leaking in through the side lobes. In adaptive cancellation, a low gain auxiliary antenna connected to the second receiver is pointed towards the interference source RFI_{ref}. The interference signals from both receivers are correlated, and followed up by an adaptive filter, which will estimate the correlation in real-time.

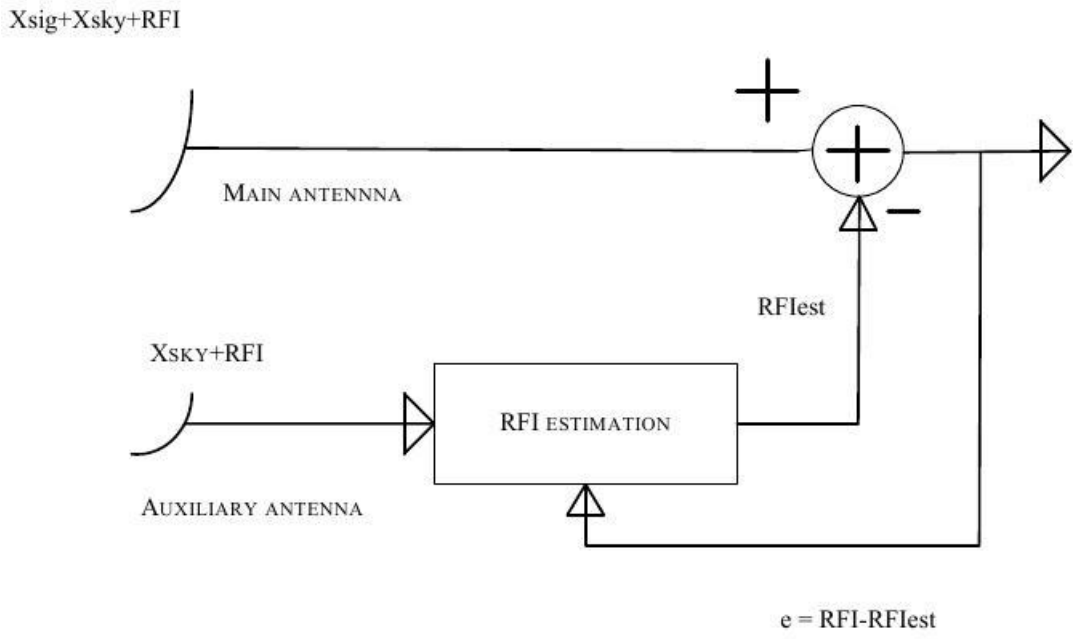

Figure 4.2: The principle of adaptive cancellation.

The adaptive algorithm compares the previous sample to the current sample and sends an update to the digital filter. In other words, the adaptive filter aims to cancel out the effect of the different propagation paths, so that the error signal $e = RFI_{main}\text{-}RFI_{ref} \rightarrow 0$, and only the X_{sig} will remain. The adaptive cancellation method is illustrated in Figure 4.2,[21],[19].

4.2.4 Kurtosis

Real-time detection and excision of the RFIs from radio astronomical data with Spectral Kurtosis (SK), has been proven to be so effective, that it may become a standard for the next generation radio telescopes. In Spectral Kurtosis, the traditional square-law detector is replaced with a Kurtosis-based RFI detector, which provides measurements of the higher order moments of the signal amplitude. The ratio R of the fourth moment m_4 and the second moment squared m_2^2 is calculated for each spectral channel, see Equation (4.3). For a radio signal with a Gaussian distribution, like the observed celestial radiation, the ratio of the moments is R=3. Deviation from this value will indicate a presence of a non-Gaussian RFI.[24]

$$R = \frac{m_4}{m_2^2}, \tag{4.3}$$

Now we present a more detailed example of the functioning of Spectral Kurtosis algorithm utilized in SK IBOB FPGA, see Figure 4.3,[25, pp. 560-572]. The SK estimate is created by Equation (4.4) to create thresholds for the data, where the S_1 and S_2 are the power spectral density (PSD) estimates in the spectral domain over a given period of time in each spectral channel k, see Equation (4.5) [25, pp. 560-572].

$$SK_{est} = \frac{M+1}{M-1}(\frac{MS_2}{S_1^2} - 1). \tag{4.4}$$

$$S_1 = \sum_{m=1}^{M} P_k, S_2 = \sum_{m=1}^{M} P_k 2, \tag{4.5}$$

where M is the number of samples. The variance for signals with Gaussian distribution, is determined by Equation (4.6). The thresholds for the SK estimate are determined by Equation (4.7).

$$.Var(SK) =\simeq \frac{4}{M}. \tag{4.6}$$

$$SK = 1 \pm \sigma^2 = 1 \pm \sqrt{Var(SK)}. \tag{4.7}$$

The spectral channel k is considered to have a presence of RFI if, $\mid SK - 1 \mid \geq \frac{6}{M}$ [25]. In Figure 4.3 all the values exceeding the threshold are flagged as a RFI. Figure 4.4 illustrates visually the the flagging and the removal of non-Gaussian data (RFI). Figure 4.4 d) shows the average spectrum in 500-1000 MHz band containing loads of RFI. Figure 4.4 a) visualises the RAW full-resolution spectrum at the full 244 kHz resolution including the RFIs. In Figure 4.4 b) is the full-resolution clean spectrum, where all the spectral channels exceeding the threshold are blanked. Figure 4.4 c) shows the clean rebinned spectrum at the target resolution of ≈1 MHz, formed by averaging in frequency by factor 4. Now four contiguous frequency bins are added and the sum is divided by the number of unflagged bins. If we look closer at Figure 4.4 b) we see that some of the RFIs around 877 MHz have escaped detection, as well as a few isolated points between 903-928 MHz from a highly intermittent RFI source. We can see, that the described mitigation method here is highly effective in removing the RFIs from the spectrum, yet a few RFIs were able to deceive the algorithm by mimicking Gaussian noise statistics.

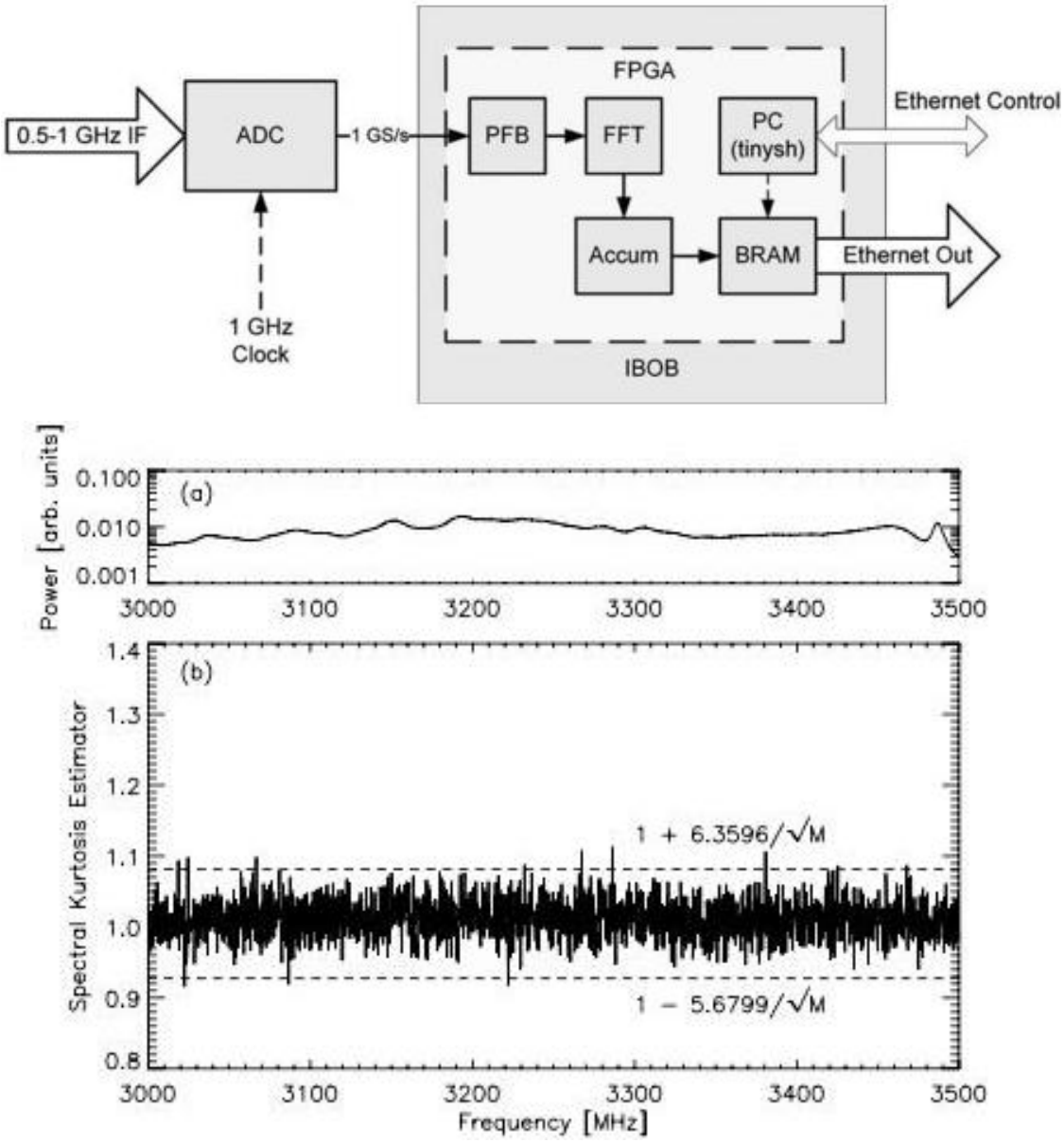

Figure 4.3: The block diagram of Spectral Kurtosis spectrometer IBOB FPGA (left). On the right (up) is a clean astronomical data with no RFI present (3000-3500 MHz) and below is the corresponding SK estimate and the thresholds (M=6104).[25]

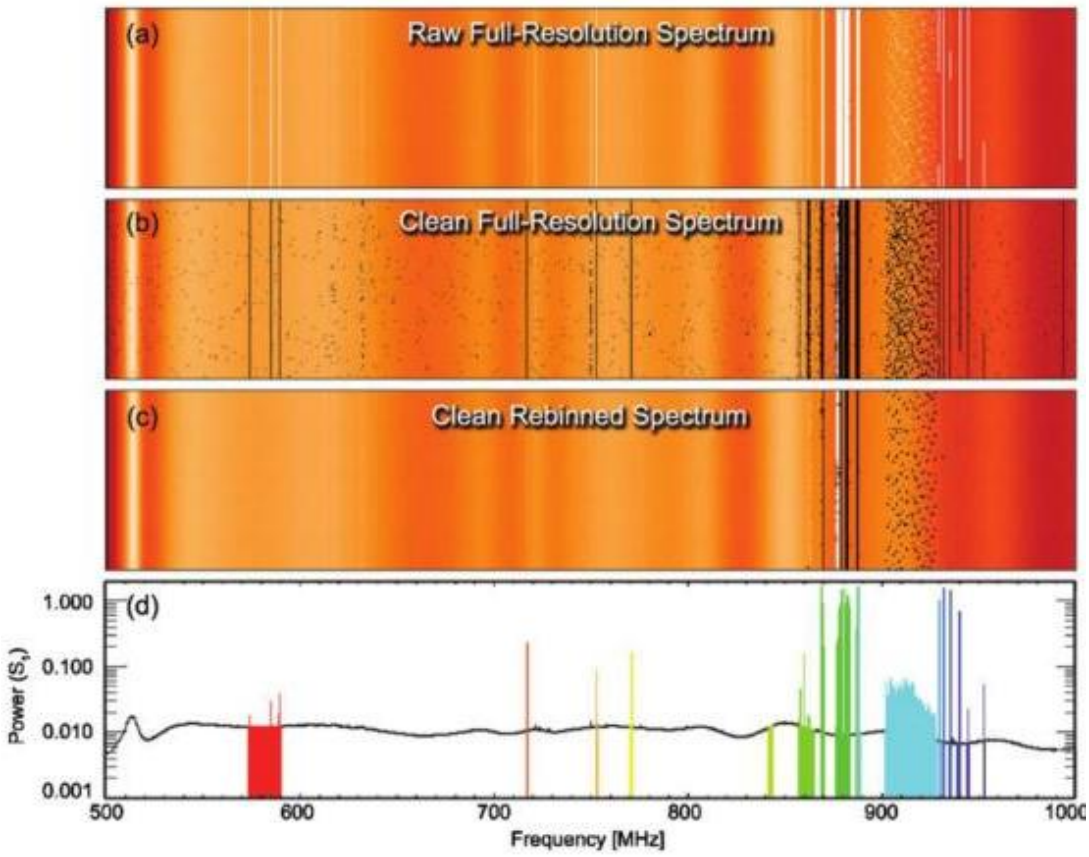

Figure 4.4: a) Raw full resolution spectrum. b) Clean full resolution spectrum. c) Clean rebinned spectrum. d) Average spectrum (500-1000 MHz). [25]

Chapter 5

RFI measurements in Metsähovi

Chapter 3 introduced a RFI-monitoring equipment utilized in INAF along with a few RFI measurements from the other observatories around the Europe. This chapter introduces the corresponding RFI-monitoring system employed in Metsähovi Radio Observatory (MRO) and also present the steerable RFI-monitoring equipment used for the external RFI studies in this thesis. Internal radio frequency interference sources in the observatory grounds were also measured and identified to determine their harmfulness in astronomical observation.

5.1 RFI-monitoring system

The radio frequency environment has been monitored in the MRO since the year 1998. The data has been gathered in a 400-2000 MHz frequency band from four cardinal points with vertical polarization. Unfortunately the RFI- monitoring setup has changed slightly over the years due to instrument breakdowns, which makes annual RFI data comparison uneasy. The present RFI equipment in the MRO consist of a log-periodic antenna LPD 500-2000, with an approximately +6 dBi antenna gain between 400 MHz...2000 MHz. The RFI antenna is installed on a rotating pole on the roof of the east wing of the observatory building, roughly on the same height as the actual radio telescope, which is located circa 20 meters away. The received RF signals are amplified with Mini Circuit ZX60-2531M-5 amplifier with +30 dB gain in the observed frequency band before the detection. The RF signal is conducted from the antenna to the detector with a Suhnex Sucoflex RG-214 coax cable with an attenuation of a 0.4 dB/m in 2 GHz. An Agilent Technology Fieldfox spectrum analyser (4 GHz) is used for detection in this system. It is run by a controlling software in a computer connected to the spectrum analyser with

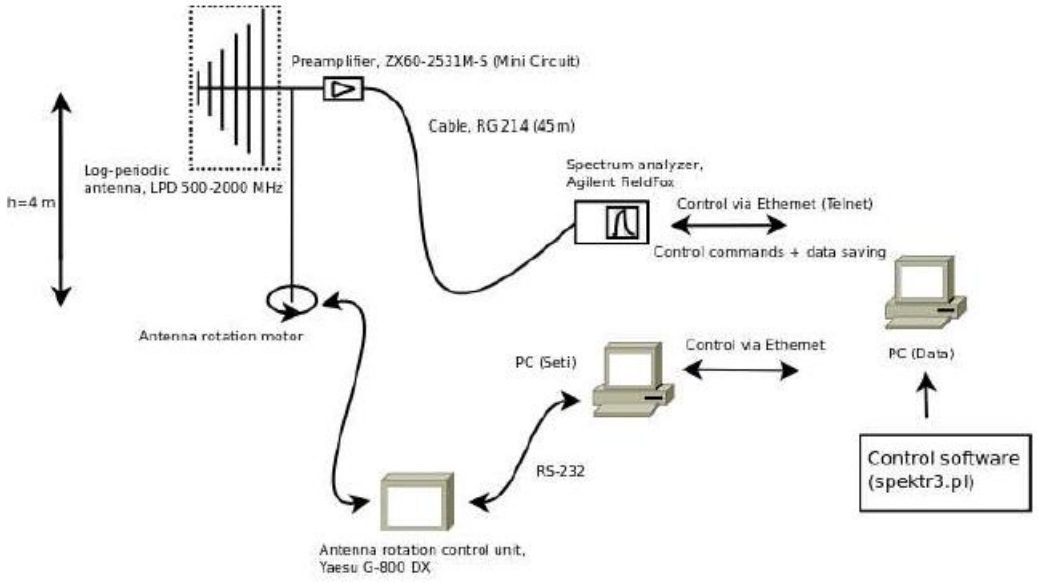

Figure 5.1: The schematics of the RFI-monitoring system in Metsähovi Radio Observatory (up). Log-periodic antenna LPD 500-2000 mounted on a rotating pole. The spectrum analyser used for RFI monitoring is an Agilent Technology Fieldfox 4GHz . [26]

an Ethernet-cable. The schematics of the RFI monitoring system are illustrated in the Figure 5.1. The applied RFI observation band covers the IF bandwidth of the radio receivers employed in the MRO. This particular band is divided into sixteen 100 MHz bands, each band is scanned ten times with spectrum analysers with max hold option. The RFI data is gathered from a four antenna position, which are the principal compass points. The complete scan consist of 64 individual scan using 3 kHz resolution bandwidth and 1 kHz video bandwidth. The sweep duration for one scan is 6,1 seconds, containing 1000 measure points [26]. The weakest detectable signal levels with this monitoring equipment are between -130...-140 dB(W/m^2/Hz).

5.2 Steerable RFI-monitoring system

A steerable RFI-monitoring system was built in the summer of 2010, approximately 70 meters away from the radio telescope due north-east. The new monitoring system visible in Figure 5.2, was built to gather more directional and wideband information about the ambient radio environment. The RFI-monitoring system is located on

the roof of a small shack circa 3.5 metres above the ground in a relatively open area with no solid obstacles blocking the view. A parabolic dish 120 cm in diameter was attached into a steerable platform, where a log-periodic antenna was mounted with a piece of a curved Finnfoam on the focal point of the dish. The focal point was calculated by Equation (5.1), [27, Chapter 4]

$$f = \frac{D^2}{16d}, \tag{5.1}$$

where D is diameter and d is the depth of the dish. The focal point of this dish is in 47 cm. In these measurements two different PCB antennas were used depending on the measured frequency band, 350 MHz-1000 MHz and 800 MHz - 2600 MHz. SMA PCB Mount was soldered on the log-periodic antennas to make coax cable use possible. Using 2 m long Suhner sucoflex coax cable, the antenna was connected to a Miteq AM-3A-0515 amplifier with a +30 dB gain in the signal band. The amplifier biasing was implemented with two Mini-Circuits ZFBT-4R2G Bias-Tees, 8 m long Suhner coax cable and a power source to provide the 15 V bias voltage. An Agilent Technology EXA spectrum analyser was used for signal detection with 300 kHz resolution- and video bandwidth. The data was recorded with a portable computer during the chosen period of time with a max hold option. The data was collected the same way as in the older RFI monitor, the observed band is divided in 100 MHz slot, each containing 1000 measure points. The achieved sensitivity of the receiver is around -160..-170 dB(W/m^2/Hz).

Figure 5.2: The steerable RFI-monitor system, log-periodic PCB antenna attached into parabolic dish (left), spectrum analyser, amplifier + voltage source and a laptop for harvesting the data (right).

5.3 Data analysis

To compensate the effects of the transmission path from the results, following data analysis was utilized. According to the specifications, the attenuation of the Bias-Tee is 0.6 dB and the attenuation of the coax cable is ∼0.5 dB/m in the observation band. Rest of the parts in the transmission path have more frequency dependent behaviour and therefore their effects need to be calculated separately in the data analysis. The first frequency dependent factor in the transmission path is the antenna gain. Some manufacturers inform the antenna factor AF in the specifications instead of the antenna gain $G_{ant1}(f)$. The dependence between antenna factor and gain is presented in Equation (5.2) (left). However, in the measurement where the parabolic dish was utilized, the antenna gain $G_{ant2}(f)$ is determined by Equation (5.2) (right),[28, pp.21]

$$G_{ant1}(f) = (\frac{9.73f}{cAF})^2, G_{ant2}(f) = \frac{\pi^2 d^2 f^2}{c^2} e_A, \tag{5.2}$$

where c is the speed of light, d is the diameter of dish and e_A is the aperture efficiency, typical values for a parabolic dish vary between 0.55-0.6. In this analysis $e = 0.55$ was used for aperture efficiency. The following component in the transmission path which needs to be compensated from measurements is the frequency response of the amplifier. The frequency response was determined by connecting the amplifier between the spectrum analyser and a signal generator. Recording the frequency response with a laptop from spectrum analyser, the effects of the amplifier were easily compensated with the help of Matlab software. The applied resolution bandwidth (RB) of the spectrum analyser affects the sensitivity of the receiver according to the Equation (3.4). To be more exact, the resolution bandwidth RB needs to be substituted by the corresponding noise bandwidth, see Equation (5.3),[29]

$$B_n = \frac{1}{G_{t,max}} \int_0^\infty G_t(f) df, \tag{5.3}$$

where $G_{t,max}$ is the maximum value of the transfer function G_t. When the frequency responses of the elements in the transmission path are determined individually, the overall compensation can be done by the following formula, where P_m is detected signal level in dBm and G_{amp} is the amplifier gain, Equation (5.4),

$$spfd = P_m[dBm] - G_{amp}[dBm] + L_{cab} - 10log(G_{ant}) - 10log(RB). \tag{5.4}$$

5.4 Development of the radio frequency environment since the year 1998

The radio frequency environment in the MRO has been monitored over twelve years now, covering all the IF bands of the employed receivers. The development of the radio environment is illustrated in Figure 5.3, where the years 1999, 2003 and 2008 are compared. The data in this plot consists of the average values recorded with max hold option over a one year period. One notable change in the radio environment is the end of the Nordic Mobile Telephone telenetwork (NMT-450) in the end of year 2002. Digital Video Broadcast (DVB) begun in September 2000, which led to the end of the corresponding analogic broadcast in September 2007. The GSM-1800 network was first utilized in urban areas in the year 2000, the first signs of these broadcasts appeared in RFI data in 2001. The interference sources detected past twelve years are listed in Table 5.1.

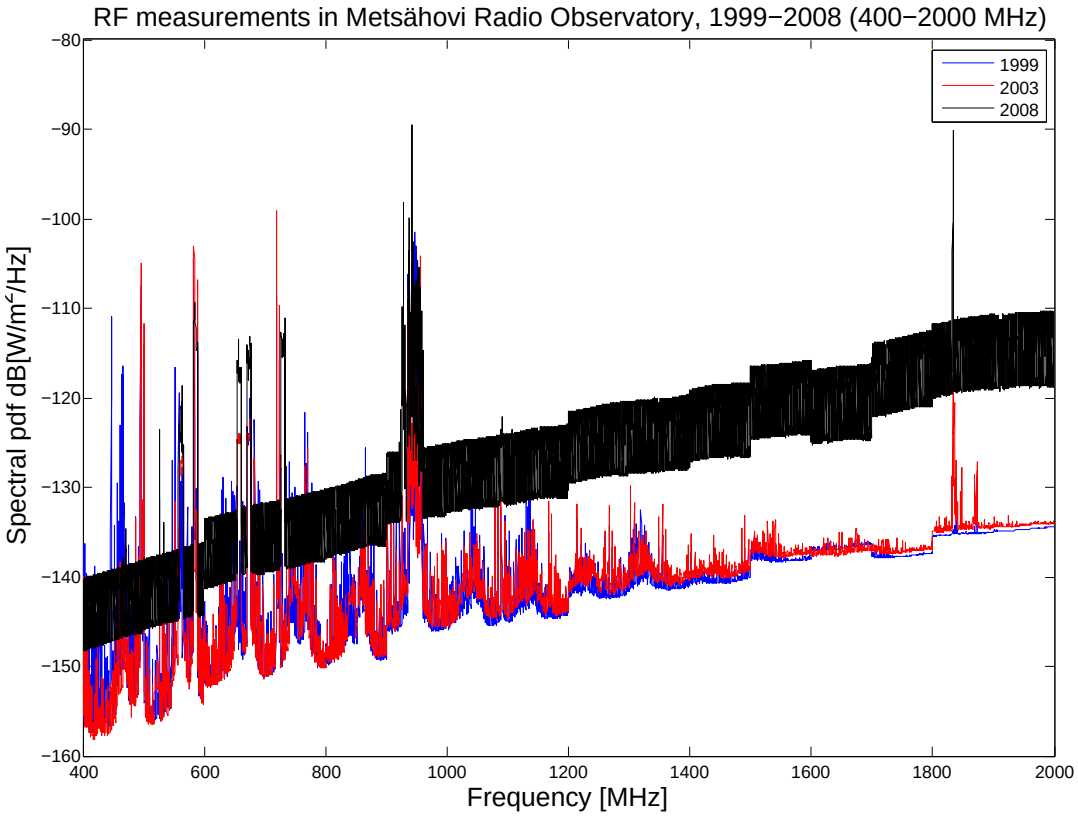

Figure 5.3: Collected RFI data from the years 1999, 2003 and 2008.

Table 5.1: List of detected radio interferences in Metsähovi.

Detected RFI Source	Frequency [MHz]	Detected spfd [dB(Wm^2/Hz)]	Description	Period of time
analog TV ch 24	498	-105	TV3	1998-2007
analog TV ch 35	586	-103	SVT	1998-2007
analog TV ch 46	674	-121	TV1	1998-2007
analog TV ch 52	722	-100	TV4	1998-2007
digital TV ch 32	562	-120	multiplex A	2000-
digital TV ch 44	658	-117	multiplex B	2000-
digital TV ch 46	674	-117	multiplex C	2000-
digital TV ch 53	730	-113	multiplex E	2000-
NMT-450	450	-115 / -128	downlink 463-468, uplink 453-458	1998-2002
GSM-900	900	-105 / -126	downlink 921-960, uplink 876-915	1998-
GSM-1800	1800	-90 / -	downlink 1805-1880, uplink 1710-1785	2001-

5.5 External RFI measurements in 2010

To gather more wideband information about the present state of the ambient radio frequency environment, a couple of new measurements were done in the summer and autumn 2010, with the equipment introduced in Chapter 5.2. To collect directional information from the surrounding radio environment the measurements were repeated by sweeping the horizon with low elevation (e$\sim 5°$) every 45 degrees. These RFI measurements were done in two different bands, 350 - 1000 MHz and 800 - 2600 MHz, with horizontal and vertical polarization. The interference sources are also identified if possible with the help of FICORAs frequency allocation.

5.5.1 RFI measurements in 350-1000 MHz frequency band

The results of the RFI measurement in the 350-1000 MHz band, from eight antenna positions with two different polarizations are illustrated in Figure 5.4. The effects

of the transmission path are compensated in the data, as explained in paragraph 5.3. Detected and identified RFI sources are listed in Table 5.2. The strongest RFI sources in this band are Digital Video Broadcasts (DVB), State Security Network (VIRVE) and GSM-900. The wideband digital mobile communication network is present in every direction in two different frequencies located around 450 and 800 MHz. Radio amateur activity in Inkoo is also clearly visible in Figure 5.4 in south-west in 432.443 MHz with horizontal polarization. All these detected interference levels naturally vary little depending on the heading, but it's clearly visible that east and south-east are the strongest directions of radio frequency interference in this band.

Table 5.2: Detected and identified RFIs between 350-1000 MHz, (FICORA).

RFI source	frequency [MHz]	Detected spfd [dB(Wm^2/Hz)]	Description
VIRVE / TETRA	394	-120	
Radio amateur	432-438	-140 - -155	Inkoo
Wideband digital mobile communication network 450	462-466	-126	
Digital TV ch 32	562	-105	multiplex A
Digital TV ch 35	586	-130	
Digital TV ch 44	658	-108	multiplex B
Digital TV ch 46	674	-108	multiplex C
Digital TV ch 53	730	-115	multiplex E
Digital TV	740-790	-125	DVB?
Wideband digital mobile communication network 800	815-840	-135	
GSM-900	900	-120 -150	downlink 921-960, uplink 876-915

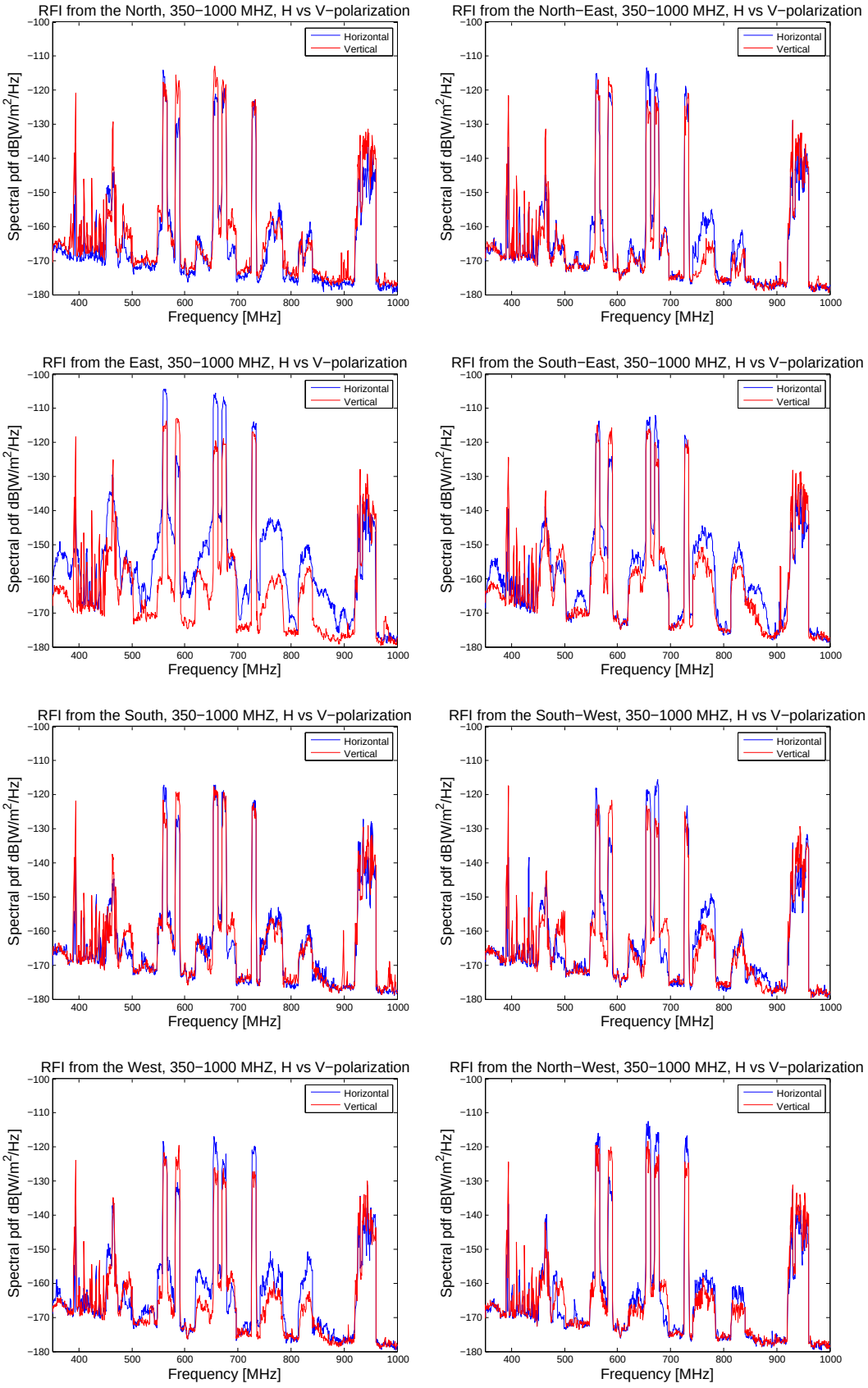

Figure 5.4: RFI measurements in 350-1000 MHz band, in every half - and principal cardinal points with horizontal (blue) and vertical (red) polarization.

5.5.2 RFI measurements in 800-2600 MHz frequency band

The second studied frequency band was 800-2600 MHz. These measurements are identical to the ones presented in Chapter 5.5.1, except that the PCB log-periodic antenna was replaced with a similar log-periodic antenna more suitable for this frequency band. Figure 5.5 illustrates the results gathered with horizontal (blue) and vertical (red) polarization from every half- and principal cardinal points. All the identified RFI sources from these plots are listed in listed Table 5.3.

Table 5.3: Detected and identified RFIs between 800-2600 MHz, (FICORA).

RFI source	frequency [MHz]	Detected maximum spfd [dB(Wm^2/Hz)]	Description
Wideband digital mobile communication network 800	790-862	-138	
GSM-900	900	-122 -115	downlink 921-960, uplink 876-915
Aviation radio traffic DME	960-1164 962-1213	-118	
Aviation radio navigation Radars	1300-1350	-152	
Iridium	1618-1630	-147	
GSM-1800	1847 1751	-132 -151	downlink 1805-1880, uplink 1710-1784
IMT (3G)	2110-2170	-142	
Microwave ove	2400-2475	-140	

The mobile phone networks GSM-900, GSM-1800 and 3G UMTS are present in every direction in Figure 5.5, with slightly chancing radiation levels. The frequency band from 960 MHz to 1213 MHz is reserved for different types of aviation radio traffic, such as, radio navigation and Distance Measuring Equipment (DME). This particular band shows significant activity with both polarizations in every direction. The following frequency band from 1300 to 1350 MHz is reserved for aviation radio navigation and radars. In Figure 5.5 this particular band is active in the directions of north, north-east, south-east, south and north-west. The only rational conclusion is that the interference shows only when an aeroplane is flying nearby. The frequency band 1400-1427 MHz is an important band for radio astronomical observation, since the hydrogen neutral line HI is located near 1420 MHz.

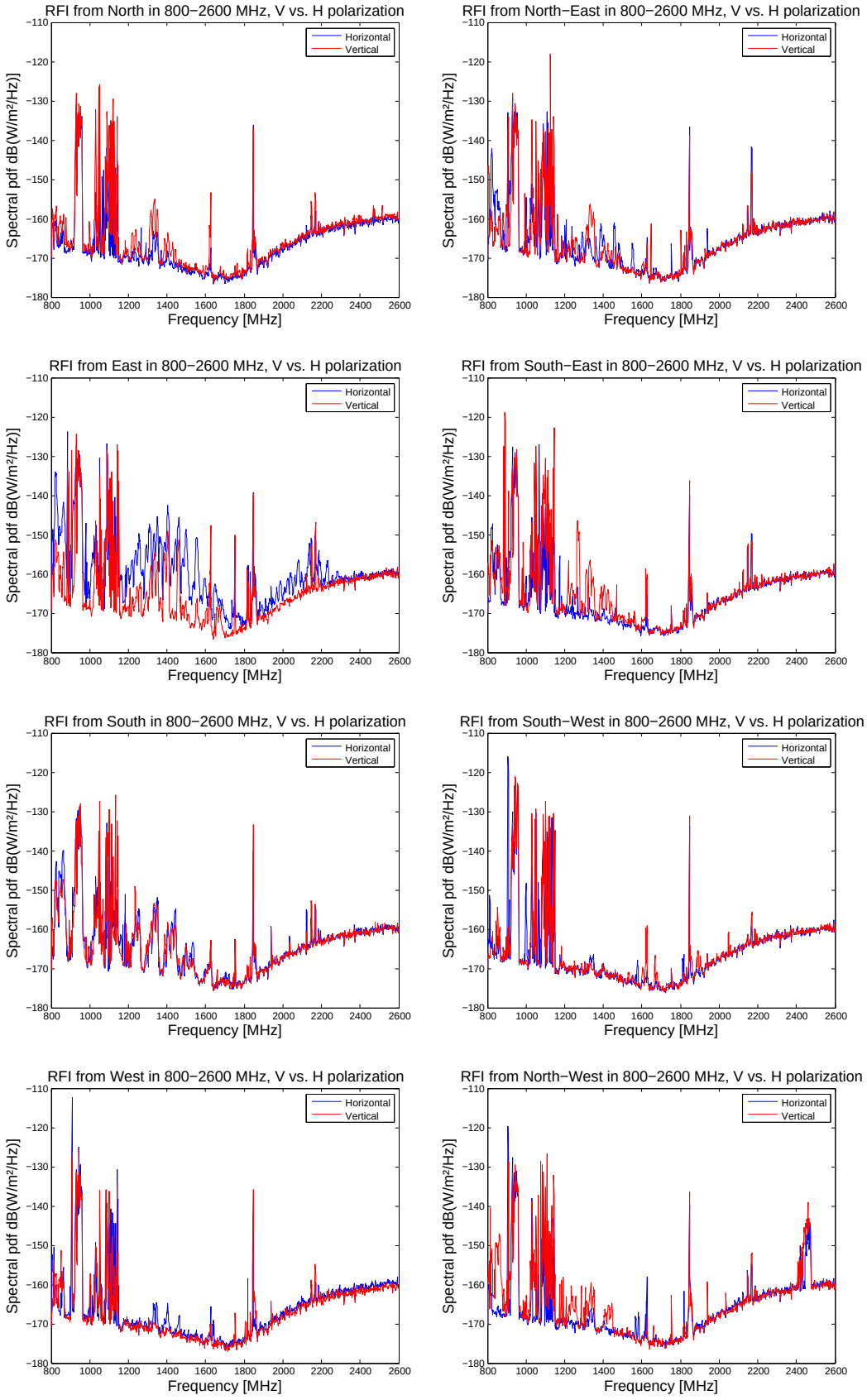

Figure 5.5: The surrounding radio frequency environment, measured in 800-2600 MHz band with horizontal (blue) and vertical (red) polarization.

This part of the spectrum is reserved for radio astronomical use only, yet there is interference detected in this band with both polarizations in north-east, east, south-east, south and north-west. The next unexpected RFI in Figure 5.5 is located around 1620 MHz. This 20 MHz wide peak is present in every direction. According to the FICORA, the frequency band 1613.8-1626.5 MHz is reserved for satellite transmissions only. The telecommunication satellite network Globalstar occupies the band 1610.000-1621.350 MHz and the satellite telephone network Iridium uses the frequency band between 1621.500-1626.500 MHz. The highest recorded spdf levels in this band were approximately -147 dB[W/m^2/Hz] with vertical polarization. In Figure 5.5 the north-western direction shows strong interference between 2400-2476 MHz. After a few additional measurements the source was identified as the microwave oven in the kitchen of the observatory.

5.6 Internal RFI measurements

Besides the external RFI, radio astronomical measurements are also vulnerable to the observatory's internal radiation. This chapter presents the results of the internal RFI measurements done inside the observatory.

5.6.1 Internal RFI measurements in 30-1000 MHz frequency band

A log-periodic antenna LPD30-1000 was placed horizontally inside the dome, shown in Figure 2.2, to measure the self-generated radiation. The antenna was set only a few meters away from the 14 m radio telescope and approximately 10 meters away from the control room, where all the computers and the measuring equipment are located. The antenna was connected to an Agilent Technology EXA spectrum analyser with a 2 m long Suhner coax cable, the effects of the transmission path were cancelled from the measurements. The data was recorded with a laptop during the daytime for several hours. Internal RFI measurements were done in two different bands 50-400 MHz and 30-1000 MHz, the results are shown in Figure 5.6.

The measurement illustrated in Figure 5.6, registered both the self-generated and the external radiation. To distinguish the internal RFI from these plots, the average and maximum values are plotted in the same figure. The transient nature of the internal radiation reveals most of the self-generated RFIs when the maximum and average values are compared. FICORAs frequency allocation and the measurement shown in Chapter 5.5.1 are also helpful in sorting out the origin of the interference.

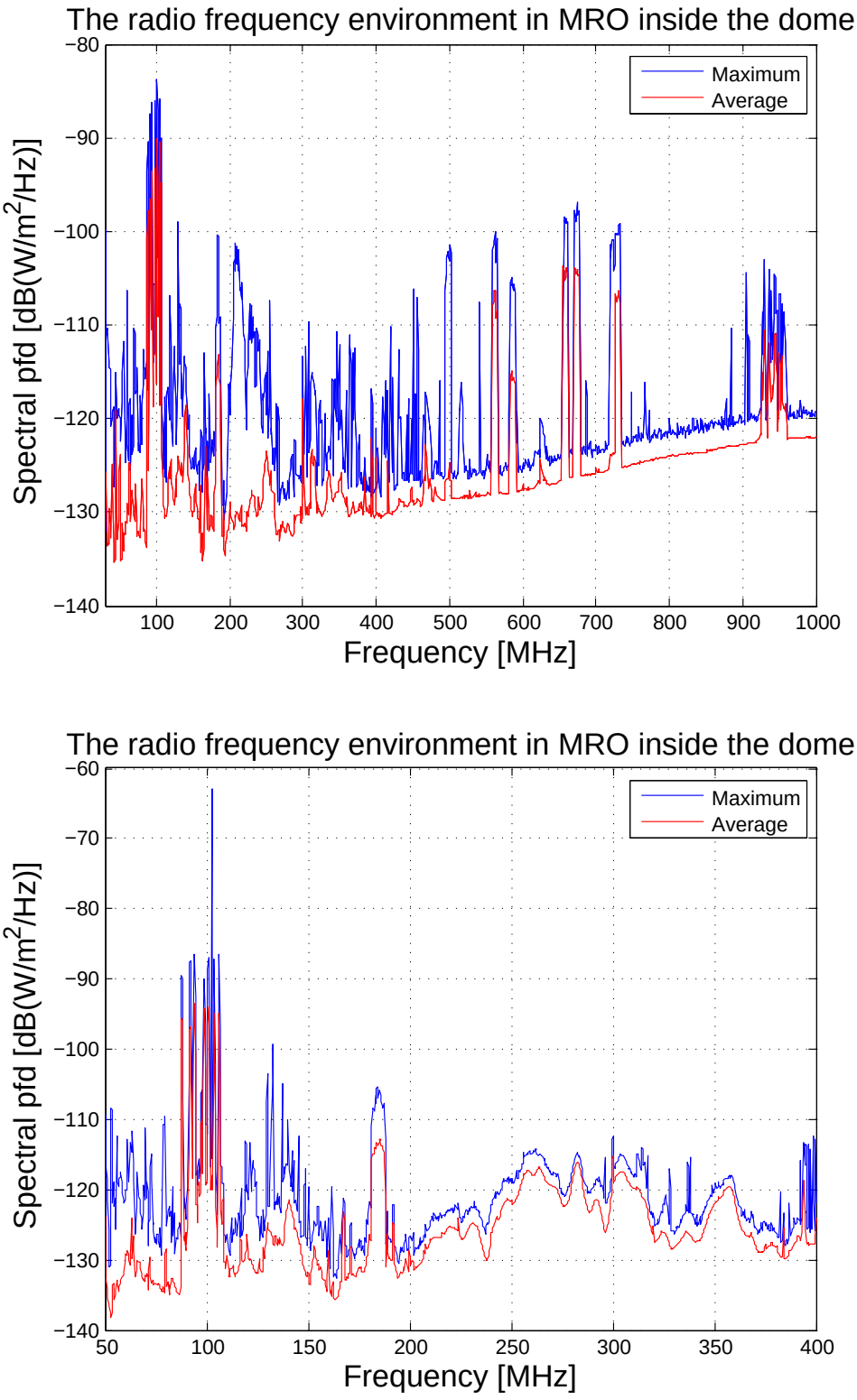

Figure 5.6: RFI inside the dome 30-1000 MHz (up) and 50-400 MHz (down).

In Figure 5.6 on the left, the frequency spectrum from 30 MHz to 87.5 MHz contains multiple narrowband interference spikes, possibly with an internal origin. The strongest interference in this measurement is between 87.5 MHz - 108 MHz, a frequency band reserved for FM-radio broadcast only. In Figure 5.6 on the right, a strong transient interference is visual at 102.55 MHz. In southern Finland there is no radio station broadcasting at this frequency, therefore the interference must have internal origin. The frequency band 108-470 MHz visible in both plots, contains loads of transient interferences with an internal origin. The following part of the spectrum until 790 MHz is reserved only for Digital Video Broadcasts, and therefore all the narrowband spikes inside this particular band are self-generated. Figure 5.6 shows also a couple of spikes between 885-910 MHz, which is reserved for GSM-900 uplink. Mobile phones are one of the most significant sources of internal radiation, therefore their use ought to be prohibited in the observatory grounds along with radio transmitters of all kind.

5.6.2 Internal RFI measurements in the 800-2600 MHz frequency band

The internal RFIs were also measured in the 800-2600 MHz band, by placing a log-periodic PCB antenna inside the control room where most of the scientific instruments are located. The data was collected during the office hours for several hours, with a spectrum analyser and a laptop. The following spectrum was recorded, see Figure 5.7. The self-generated radiation can be identified the same way that was described in the previous paragraph, therefore the maximum values(blue) and the average values (red) are compared in the plot.

By far the strongest interferences in this band are the spikes at 891.5 and 900 MHz, which belongs to GSM-900 uplink. The frequency band between 960-1240 MHz is reserved for different types of aviation radio broadcast, which typically are intermittent in nature, that's why it's hard to distinguish the origin of the interference spikes in this part of the spectrum. Weak, but constant RFI is detected at 1498 MHz, this frequency spike is absent in the external RFI measurements of Chapter 5.5.2, and therefore it must have an internal origin. The source of the wideband interference between 2410-2480 MHz is the microwave oven used in the kitchen during lunch time, circa 20 meters away from the measuring antenna.

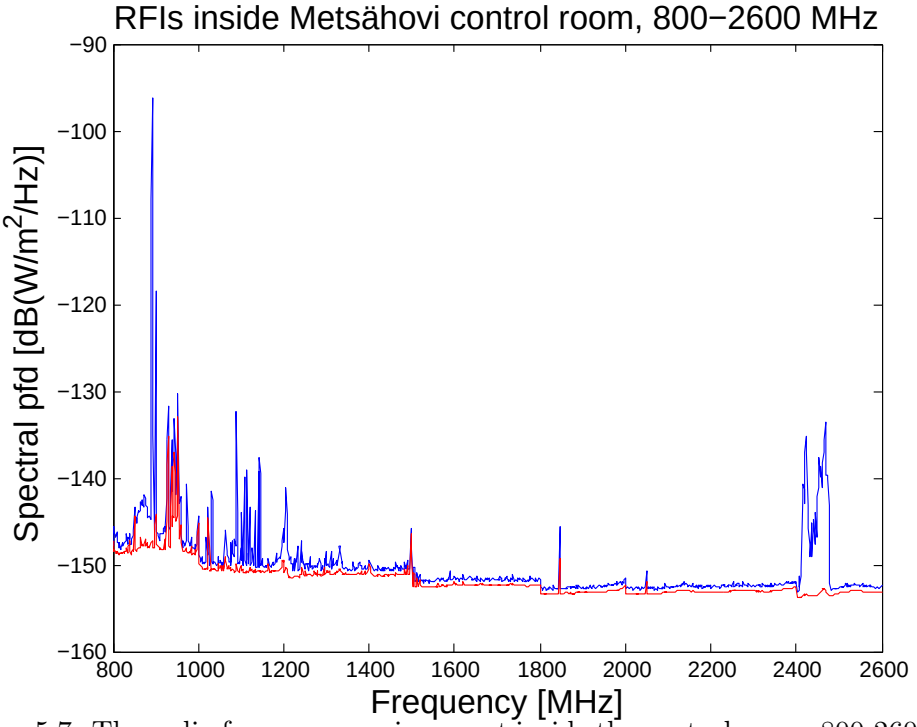

Figure 5.7: The radio frequency environment inside the control room, 800-2600 MHz band.

5.7 Harmful internal RFI sources

The previous Chapter 5.6 showed us that the self generated RFIs are also a significant threat to astronomical measurements. Some of these radiating equipment are obligatory for astronomical studies, and therefore their use cannot be banned. In this chapter, we present a couple of these radiating devices and measure their unwanted radio emissions.

5.7.1 Hydrogen maser

One mandatory equipment for the radio observatories is the hydrogen maser, which is used in a VLBI session. Unfortunately this piece of equipment is also a wideband source of interference and therefore needs to be shielded inside a Faraday cage. In the MRO the hydrogen maser is placed in a bunker inside of a Faraday cage circa 20 meters away from the telescope. Figure 5.8 shows the wideband interference radiated by the maser between 1-6 GHz. The measurements were done with a log-periodic- and Vivaldi-PCB antenna connected to the spectrum analyser. The distance between the source and the antenna is here less than one meter.

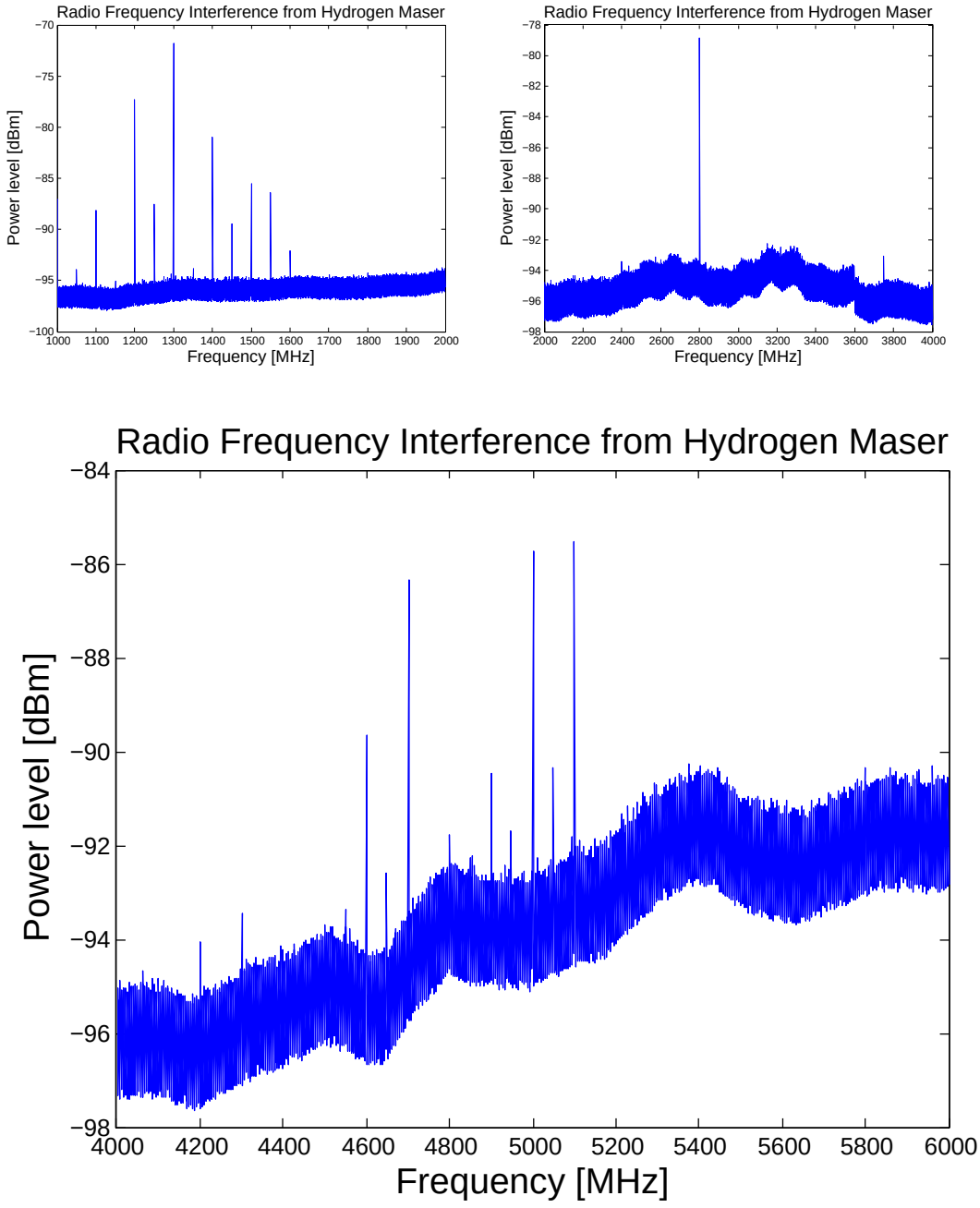

Figure 5.8: Radio frequency interference radiated by the hydrogen maser in the MRO.

5.7.2 Microwave oven

Microwave ovens are by far the strongest source of internal radiation. In Metsähovi, the radio observatory is not the only building in the area with a microwave oven. Buildings belonging to the Finnish Geodetic Institute also lie in the MRO grounds, and also have a microwave oven. The nearest outside settlement, which might have a microwave oven is 500 m away due north. Radiation from the microwave ovens in the observatory grounds were measured with the steerable RFI monitor presented in Chapter 5.2. Measuring antenna is located circa 30 meters away from the building belonging to the Finnish Geodetic Institute and 70 meters away from the radio observatory's kitchen. During these measurements, the microwave ovens were turned on one at the time. Figure 5.9 illustrates the magnitude of this interference compared to the surrounding radio environment. These tested microwave ovens are strong wideband radiators between 2400 - 2470 MHz. The S-band receiver used for geodetic measurements has a RF bandpass filter 2210 - 2350 MHz. Even if the interference from these microwave ovens is attenuated enough by the bandpass filter, it still might cause saturation in the performance of the front end Low-Noise-Amplifier (LNA). Use of these microwave ovens ought to be prohibited during the S-band measurements.

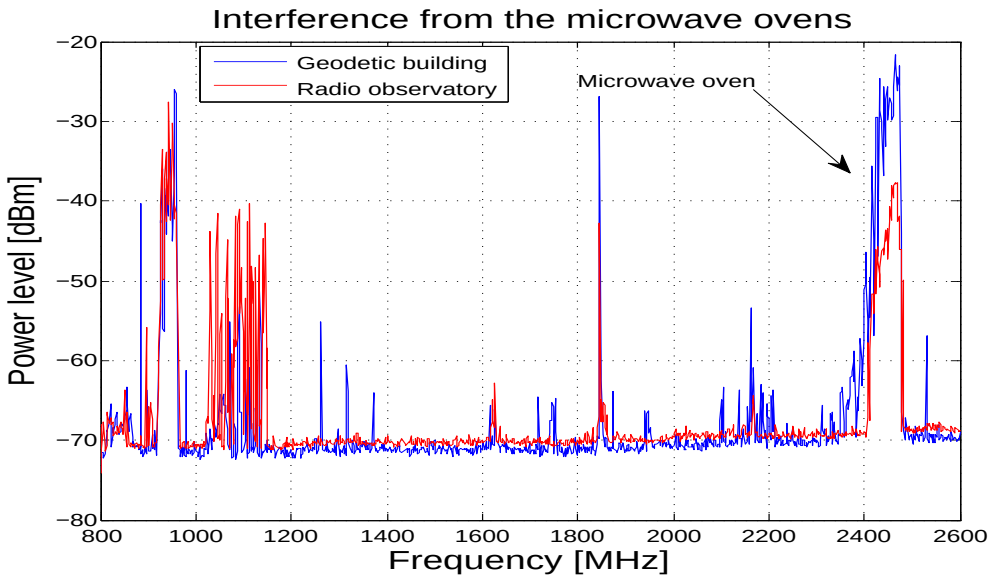

Figure 5.9: Radiation from the microwave ovens in the MRO compared to surrounding radio environment, in 800-2600 MHz band. Antenna pointed toward the geodetic building (blue), and toward the radio observatory (red).

5.7.3 RFI from mobile phones

Mobile telephone networks in Finland have changed rapidly since early days of the NMT-450. Nowadays the existing digital cellular systems are GSM-900, GSM-1800 and UMTS (3G), which all are present in Metsähovi, see Figure 5.5. The GSM-900 and 1800 networks are not directly threating any of the MRO astronomical receivers in the signal band, but if they are used next to the receiver or inside the control room, they might cause distortion by leaking in to the IF-channel. Figure 5.10 illustrates the uplink- and down-signals of GSM-900, measured with log-periodic PCB antenna and a spectrum analyser circa 3 meters away.

The narrow spike at 906 MHz is the uplink signal from the mobile phone and the 921-960 MHz is the downlink band. According to the Finnish Radiation Safety Centre (STUK), when mobile phones are operating in a remote location, such as Metsähovi, they send out their maximum power to establish good connection with the nearest base station. These Maximum powers vary from 0.25 W (GSM-900) to 0.125 W (GSM-1800). When the mobile phone uses the General Packet Radio Service (GPRS) for data transmission, the power levels can be triple compared to the GSM-900. UMTS (3G) network operating in 2110-2170 MHz frequency band, covers almost all the urban areas in Finland. This network is present in every direction in the external RFI measurements, see Figure 5.5. This application is a growing threat to the geodetic S-band measurement, since it operates only 30 MHz away from the signal band of the receiver. The effects of this 3G-network in S-band observation are clearly visual in Chapter 6.1.

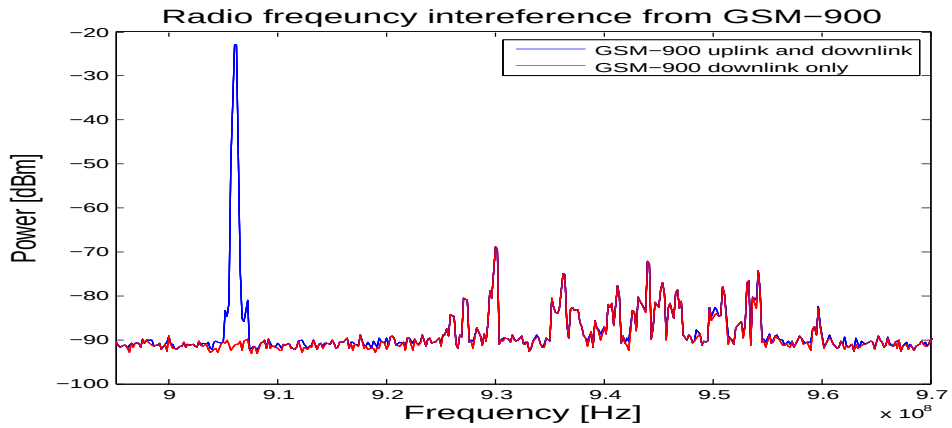

Figure 5.10: Interference from a mobile phone (GSM-900).

5.7.4 Ground - and Wall Penetrating Radars, GPR and WPR

The Metsähovi radio observatory shares it's grounds with the Finnish Geodetic Institute. Researchers from the Geodetic Institute occasionally probe the ground and the soil, with Ground- and Wall penetrating Radars (GPR and WPR). Since these gadgets are used in close proximity of the radio telescope, their undesired radio emissions were measured. Table 5.4 lists all the tested radar equipments and their operating frequencies.

Table 5.4: Ground and wall penetrating radars and their operating frequencies used by the Finnish Geodetic Institute in Metsähovi.

Radar type	Operating frequency
Ramac CU II GPR	250 MHz
Ramac CU II GPR	500 MHz
Ramac CU II GPR	800 MHz
Ramac CX WPR	1600 MHz

The unwanted radio emissions from these radars were measured with a spectrum analyser and a log-periodic PCB antenna held only a few meters away from the radars. Figure 5.11 illustrates the radiation from these radars in a narrow span, when the antenna of the radar was pointed toward the measuring antenna. In normal use, the radars are pointed towards the ground where they emit most of their energy. In these measurements, it was noticed that these radars leak radiation as soon as the power is turned on, even though they are on idle. Figure 5.12 shows the radiation from the Ramac CX 1600 MHz WPR, when the radar is pointed towards the ground. This measurement was done approximately 30 meters away from radar. The background radiation is plotted on red, to indicate more clearly the amount of radiation this radar is leaking. The maximum value of the unwanted emission power is 15 dBm above the noise floor. Because these radars are operating at such low frequencies, they don't interfere with the astronomical measurements directly. Strong enough radiation can penetrate the shielding of the receiver chain in some point and corrupt the astronomical measurements in the IF-channel. In the MRO, solar observation is done with low frequency log-periodic antenna between 170-870 MHz. This radio receiver will suffer from the unwanted radio emissions from the radar, and therefore the MRO should be notified before using the radars in the observatory grounds.

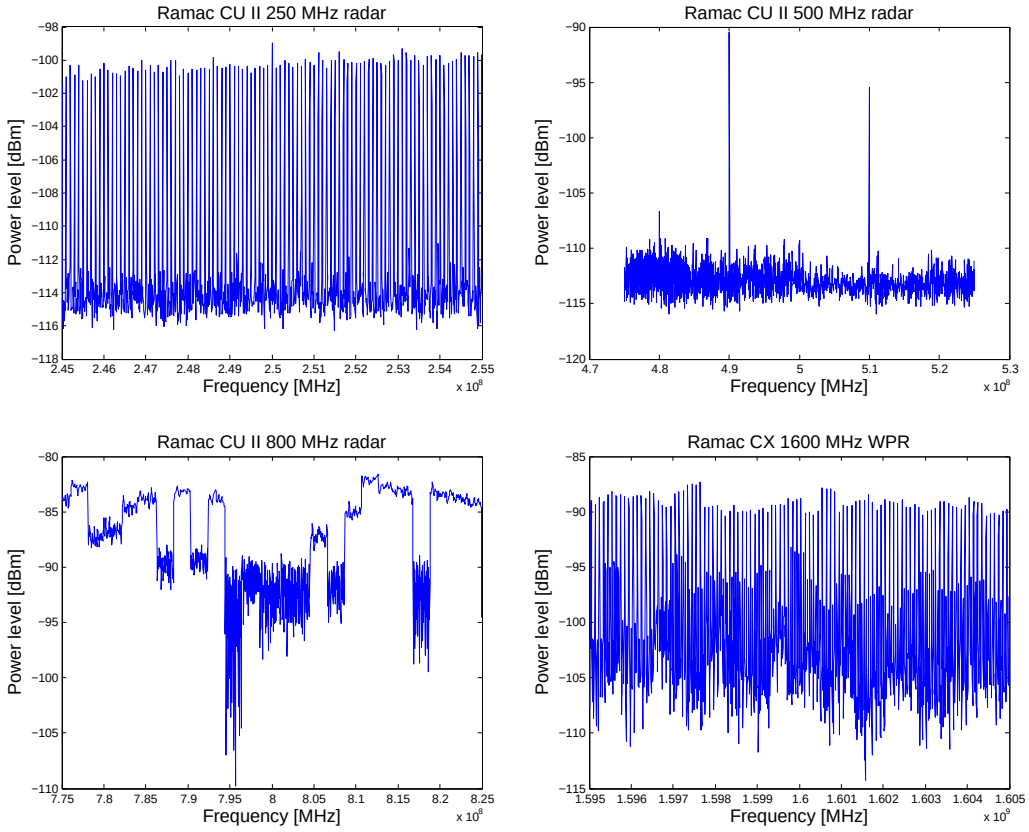

Figure 5.11: Unwanted radio emissions from the tested Radars. Distance between the radar and measuring antenna only a few meters.

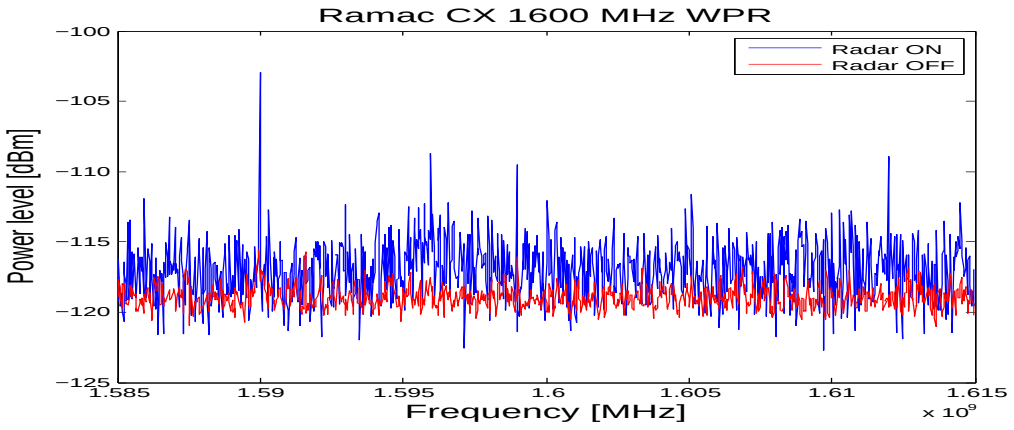

Figure 5.12: Ramac CX 1600 MHz WPR pointed towards the ground, measuring antenna circa 30 meters away.

Since these radars are used in close proximity of the radio telescope, 20...100 meters, the damping of the radar operating frequencies are estimated individually. Figure 5.13 illustrates how these unwanted emissions are damped by the free space loss, according to Equation (5.5) [30, pp. 425], where d is distance and f is the radar frequency.

$$L = 20log(\frac{4\pi df}{c}), \tag{5.5}$$

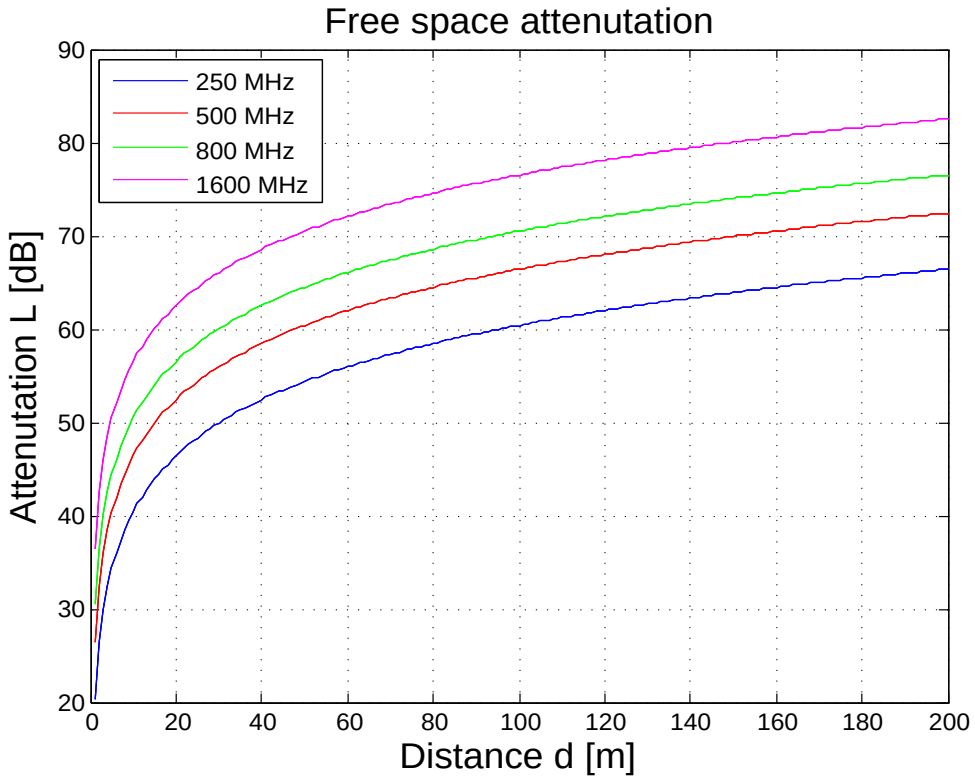

Figure 5.13: Free space attenuation at the radar's operating frequencies.

5.7.5 RFI from scientific instruments and experiments

The use of other scientific instruments can also cause significant amounts of harmful radiation. Signal generators and spectrum analysers are used in various scientific experiments, where they work basically as a radio transmitter. In Chapter 5.6.1 the internal radiation inside the MRO was measured in 30-1000 MHz band. During one of these measurements, a spectrum analyser was set to measure the return loss of an antenna, in the workshop circa 20 meters away from the measuring antenna. Later in the RFI data analysis an unexpected interference was discovered, which turned out to be the spectrum analyser sending out wideband radiation through the antenna between 175-800 MHz. Figure 5.14 illustrates the significant amount of this radiation, transmitted by the spectrum analyser in the next room (blue line).

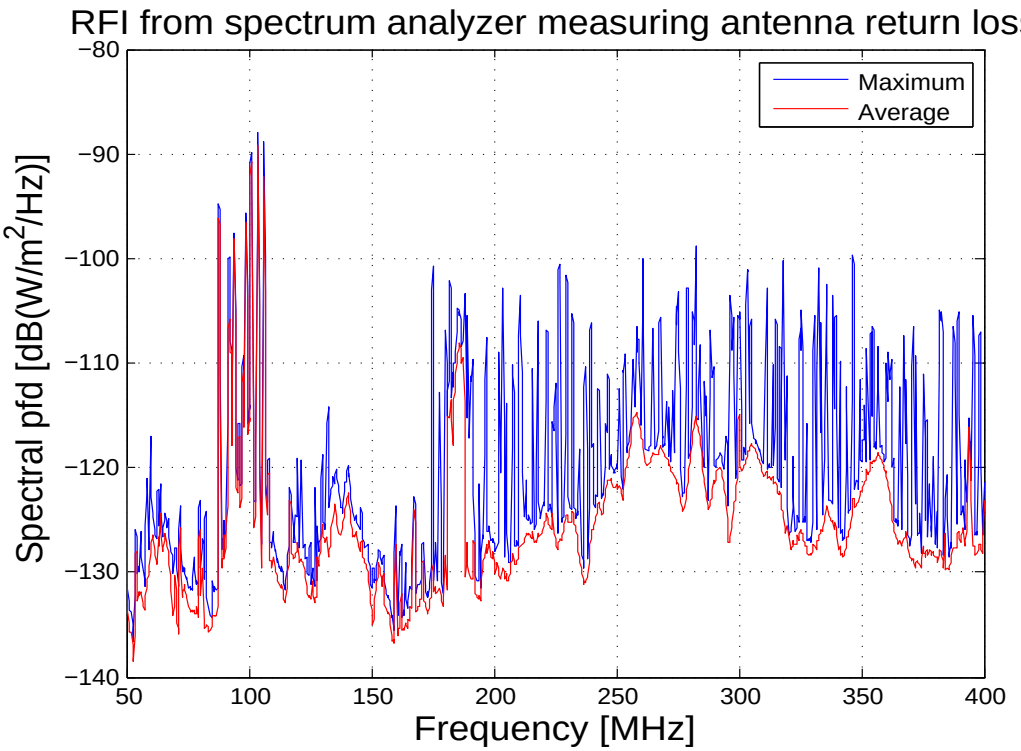

Figure 5.14: Interference from a spectrum analyser measuring the return loss of an antenna.

The workshop, where most of the RF testing takes place is located next door to the control room, where the post-processing of the astronomical data is handled. This type of wideband radiation can affect the astronomical measurements by leaking in the IF-channel or distorting the estimates for the background radiation levels temporarily. The solar observation antenna measuring low frequencies below 1 GHz is located on the yard not more 15 meters away from the workshop, is also vulnerable to this type of radiation. The best way to protect these astronomical observations, is to move all type of RF testing inside a Faraday cage. If there is no Faraday cage available, the RF testing ought to be scheduled when no astronomical observation is under way.

Chapter 6

Astronomical radio receivers and RFI

The previous chapter presented all the detected external and internal radio interference sources in Metsähovi radio observatory (MRO). In this chapter, we investigate more closely how these RFIs affect radio astronomical observation. The best way to study these effects is to measure the receiver's IF channel with a spectrum analyser, directly from the IF port before the signal goes through further processing. Thee different astronomical receivers were tested, S-band, X-band and 22 GHz VLBI, by recording the IF-channel spectrum while sweeping the horizon with a low elevation ($e = 5°$). In another test, the radio receivers were exposed to artificial radio interference, to study the possible front end amplifier (LNA) saturation.

6.1 Geo-VLBI receiver

The Geo-VLBI receiver was mounted in its natural place in the radio telescope. The receiver was cooled down to it's operational temperature, circa 16 K. A spectrum analyser was attached to the receivers IF port with a coax cable. The data was recorded with a laptop in eight antenna positions, results are found in Figure 6.1. The reference signal (blue) in these plots, was measured, by placing the receiver inside a semi-Faraday cage, when the antenna was pointed toward an absorber cooled down with liquid nitrogen to 77 K. As we can seen from Figure 6.1, all directions show wideband interference on the rising edge of the IF channel in 636-640 MHz. Since this receiver has a superheterodyne structure, the corresponding up-converted frequency of this RFI is $f_{LO} + f_{RFI} = 2170$ MHz [2].

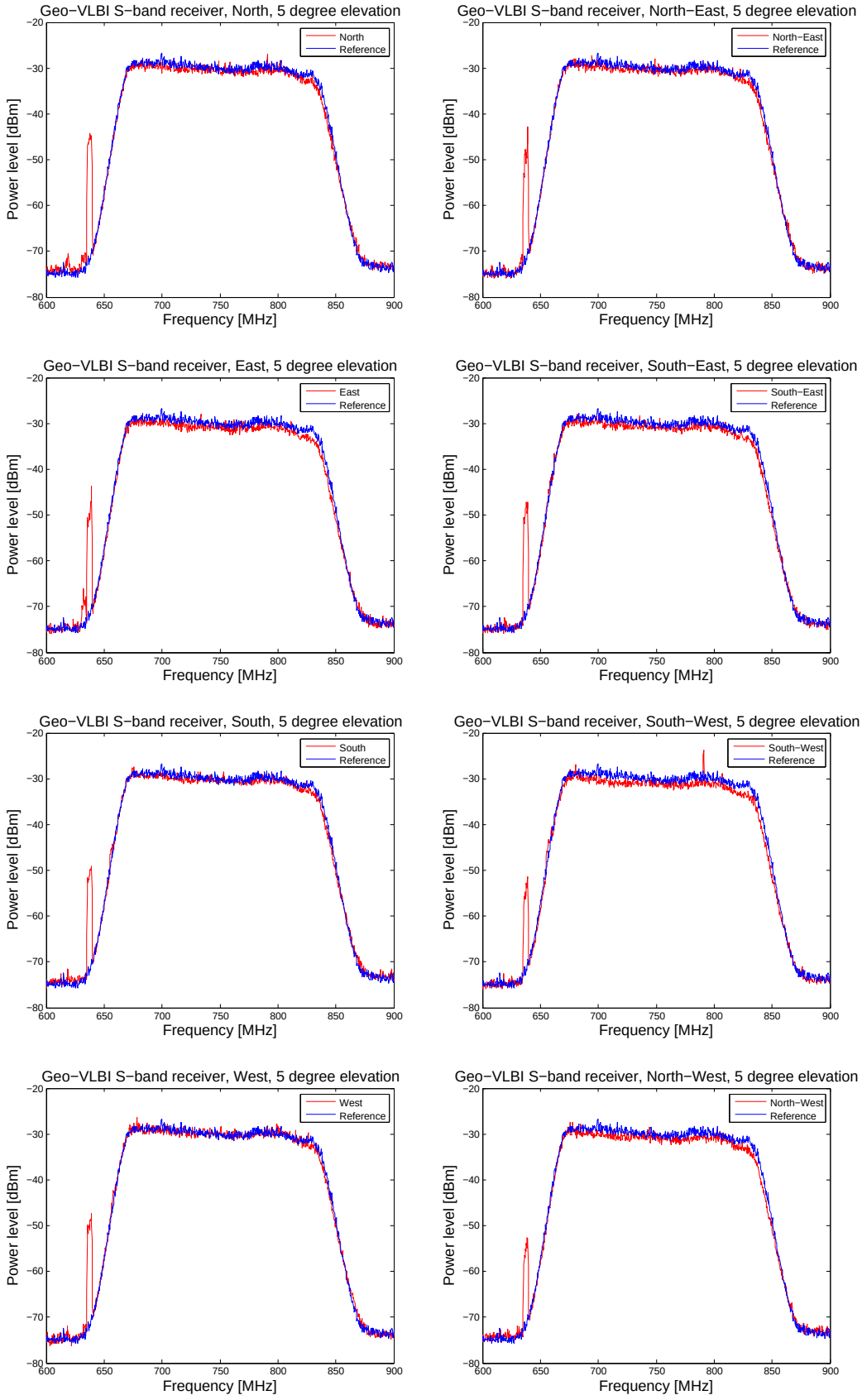

Figure 6.1: Geo-VLBI S-band receiver, IF channel recorded in eight antenna positions, elevation 5°.

The source of this interference is UMTS (3G-network). The S-band receiver in question, has suffered from sensitivity loss for a few years. The ever growing 3G activity in the area might have deteriorated the performance of the receiver. Interferences were also detected in the signal band of the receiver, see Figure 6.1 due south-west. This 7 dB spike is found at 791 MHz, the corresponding up-converted frequency is 2321 MHz. The origin of this RFI was found in Inkoo, 45 km due south-west from the MRO, where a radio amateur beacon is located. The elevation dependence of the RFIs, was tested by increasing the elevation with 10 degrees, see Figure 6.2. We can infer that the 3G signal is leaking in through the side lobes of the antenna pattern, since it doesn't show notable change in the power level with different elevations or azimuths. The radio amateur beacon, on the other hand weakens rapidly when the elevation or the azimuth is altered.

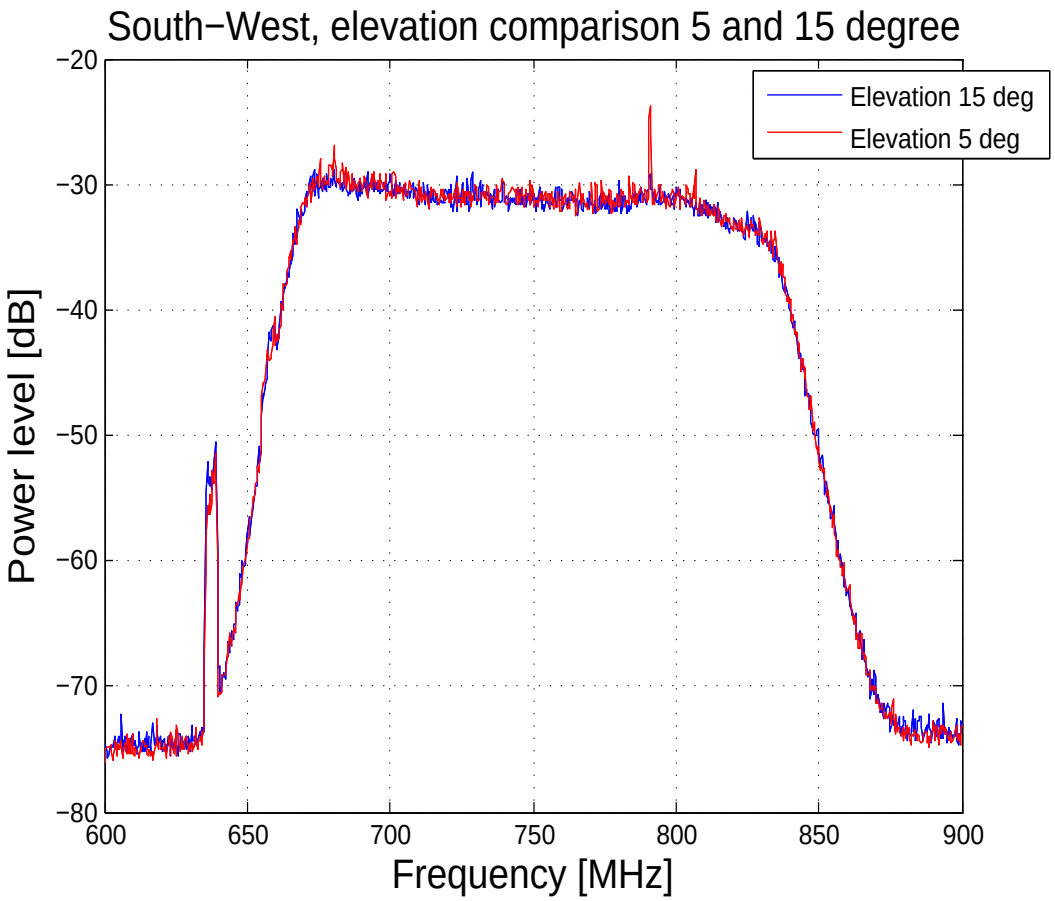

Figure 6.2: RFI elevation dependence, radio telescope pointed toward south-west.

The Geo-VLBI receivers second channel is located in the X-band, between 8.15-8.65 GHz. This part of the spectrum is free from the internal and the external radio interference. Nearby bands are reserved for radio links and military applications, none of which disturb the measurements in the MRO in X-band, as we can infer from Figure 6.3.

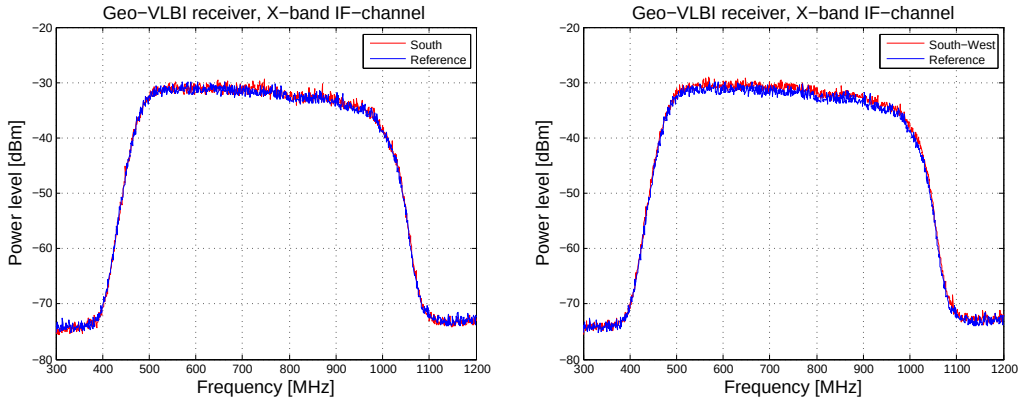

Figure 6.3: Geo-VLBI X-band receiver IF-channel, elevation 5°.

6.2 22 GHz VLBI receiver

The 22 GHz VLBI receiver was mounted in the telescope, where it was set to sweep the horizon with 5 degree elevation. The receiver's signal band lies between 21.980-22.480 GHz and the IF channel between 0.5-1.0 GHz. The IF channel spectrum was recorded in eight antenna positions, the results are visible in Figure 6.4. According to FICORA, the nearby bands around 22 GHz are reserved for, YLE radio satellite traffic 21.400-22.000 GHz, Short Range Radar system (SRR) in cars 21.650-23.600 GHz and radio links 22.078 -23.600 GHz. Figure 6.4 shows remarkable distortion in the IF-channel spectrum, when the telescope is pointed eastward. This type of distortion in the IF-channel spectrum can only be caused by a strong interference in the signal band or nearby, which is able to saturate the LNAs amplification. Some smaller interferences were also detected in the IF channel spectrum from south and south-west. The 22 GHz receiver has a relatively narrow beam width, and the observations are never done below 20 degree elevation, whereupon it's not likely that these interferences leak in through the main lobe of the antenna pattern.

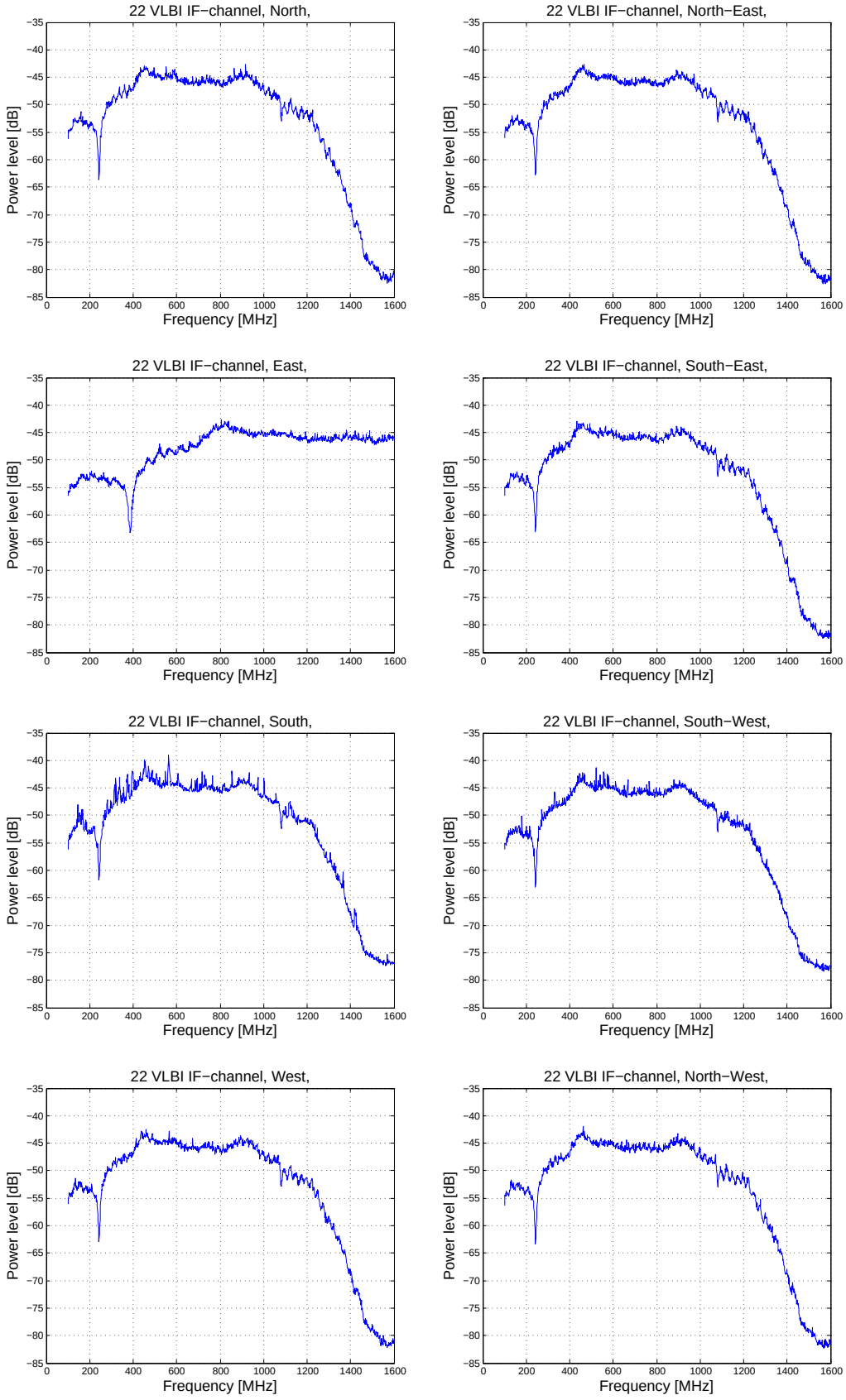

Figure 6.4: The 22 GHz VLBI receiver's IF channel measured every 45°, with 5° elevation.

The RFI tolerance of the receiver was tested with two artificial interference sources, a signal generator radiating through an antenna and a cell phone (GSM-900). In Figure 6.5 upper left corner, a cell phone was placed less than 10 cm away from the IF port of the receiver, meanwhile the other interference source was transmitting at 11.118 GHz 10 meters away from the feed horn of the radio telescope. When the cell phone was placed close enough to the IF port, the interference was able to penetrate the shielding and leave its mark in the IF channel spectrum. In the other plots in Figure 6.5, the signal generator was set to transmit interference at 20.882 GHz, 21.750 and 22.580 GHz. The interference levels in these measurements were unnaturally high, around -20 dBm to 0 dBm. None of these interference attempts were able to cause the saturation in the receiver's LNA performance, as shown in the Figure 6.4, when the radio telescope was pointed due east.

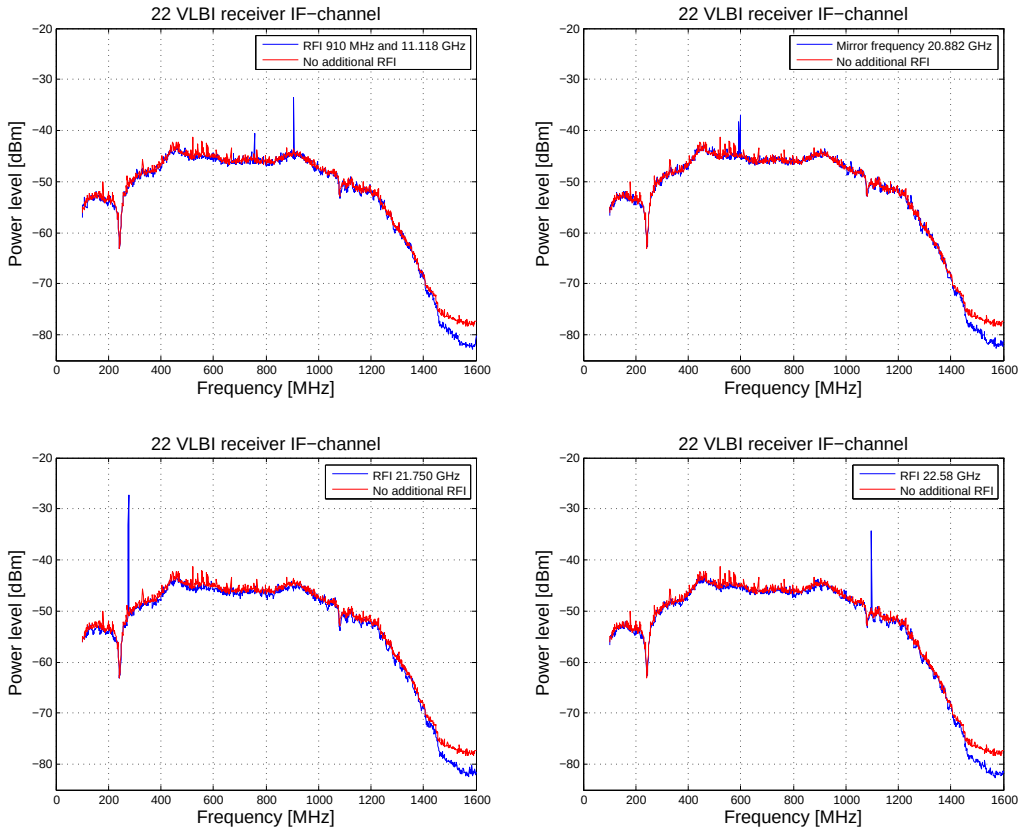

Figure 6.5: 22 GHz VLBI receivers IF-channel, disturbed with artificial RFI.

6.3 RFI in the solar observations

A new scientific instrument used for solar observations called Callisto is utilized in the MRO since the autumn of 2010. The instrument consist of a tracking antenna equipment and a Callisto software, which was set to monitor the solar activities in the 175-870 MHz band. Unfortunately this part of the spectrum is filled with ground-based RFIs, which can be seen in the Callisto spectrogram data, see Figure 6.6. The spectrogram in the upper right corner, shows clearly all the interferences in the observation band. The strongest interference sources in this particula band are the Digital Video Broadcasts. Both upper spectrograms show odd fluctuation in the data between 180-400 MHz. The origin of this interference was later discovered to be the high brightness led drivers (Micro Bridge PT4115), located all over the facility. Replacing the lighting ended the fluctuation in the Callisto data. In Figure 6.6, both spectrograms in the bottom are illustrating a radio burst in the Sun, unfortunately these measurements are distorted slightly by the radiation from the led lights.

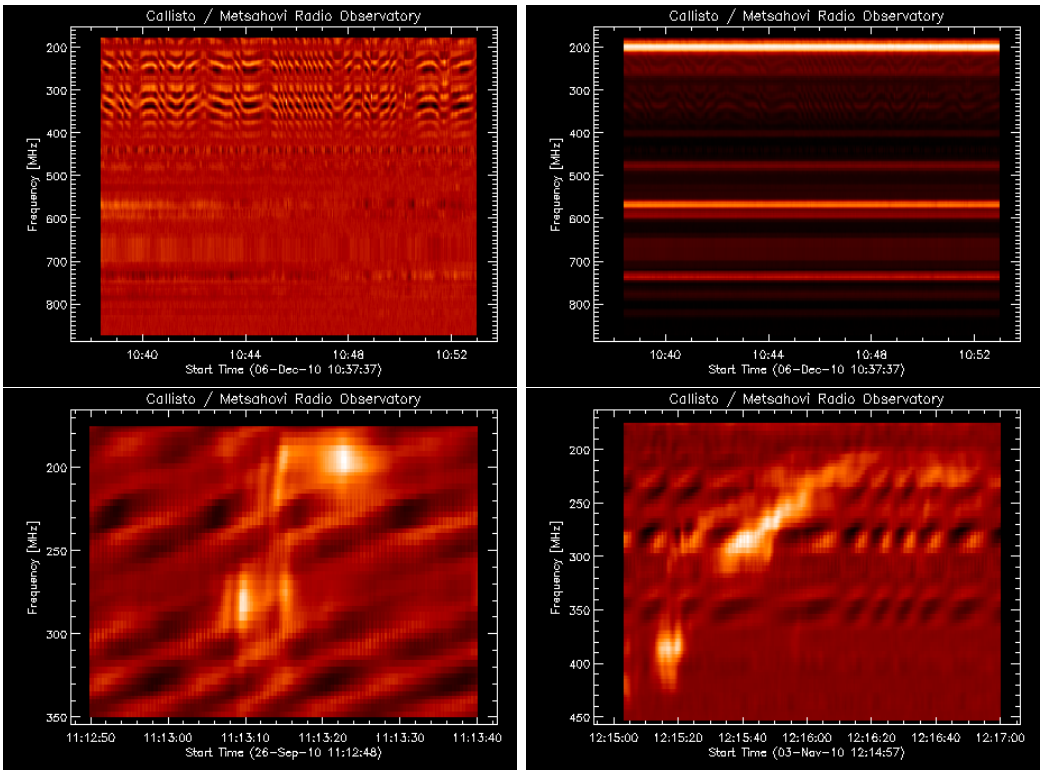

Figure 6.6: Callisto spectrogram data distorted by external and domestic interference.

Chapter 7

RFI monitoring improvements

The present RFI-monitoring system was first utilized in the MRO in the year 1998, to follow the development of the ambient radio frequency environment. The RFI monitor in question was introduced in Chapter 5.1. This chapter presents a proposal for updating the already existing RFI equipment with a few low cost improvements, to gain a wider observation band and to gather data with different polarizations. The self-generated radiation is a significant threat to the astronomical observation, therefore couple of internal RFI monitoring improvements are also presented in this chapter.

7.1 RFI-monitoring system update

The general principle in the new RFI monitor is basically the same that in the old one, with few minor changes and additions. Two log-periodic antennas, measuring horizontal and vertical polarization are attached on a rotating pole. The distance between these two RFI antennas ought to be great enough to avoid the near-field coupling of the antennas, which can be determined by Equation (7.1) [2, pp.160]

$$d = \frac{2D^2}{\lambda}, \tag{7.1}$$

where D is the dimension of the larger antenna element. All the new required components for the RFI monitor update are listed in Table 7.1. The new proposed RFI antenna is AARONIA Hyper log 4040, which has a larger antenna element of 360 mm. The reasonable distance between the antennas is approximately 3.5 meters according to Equation (7.1). Wideband low noise amplifiers (Miteq AMF-

2D-00100400-14-13P) are used for the signal amplification in this proposal. Both of these amplifiers are connected to a switch with a coax cable, from where the RF-signal is conducted to the spectrum analyser (Agilent Technoly Fieldfox 4 GHz). The spectrum analyser is guided by a computer where the data is also stored. The best way to visualize the measured RFI data from eight antenna positions with two polarizations, was introduced in Chapter 5.5.2. The effects of the transmission path should be compensated in the data analysis, as described in Chapter 5.3. It is sound to set the resolution bandwidth around ~ 300 kHz, due to the wide observation band. The rough schematics of the new RFI-monitoring system can be found in Figure 7.1.

Table 7.1: List of required instruments and their specifications for the RFI-monitoring system.

Log-perdioc antenna	
Producer	AARONIA AG
Model	Hyper log 4040
Frequency band	400-4000 MHz
Antenna gain	4 dBi
Weight	1200 g
Amplifier	
Producer	Miteq
Model	AMF-2D-00100400-14-13P
Frequency band	100-4000 MHz
Gain	26 dB
Cable	
Producer	Suhner
Model	Sucoflex RG-214
Spectrum analyzer	
Producer	Agilent Technologies
Model	FieldFox
Frequency band	Up to 4 GHz

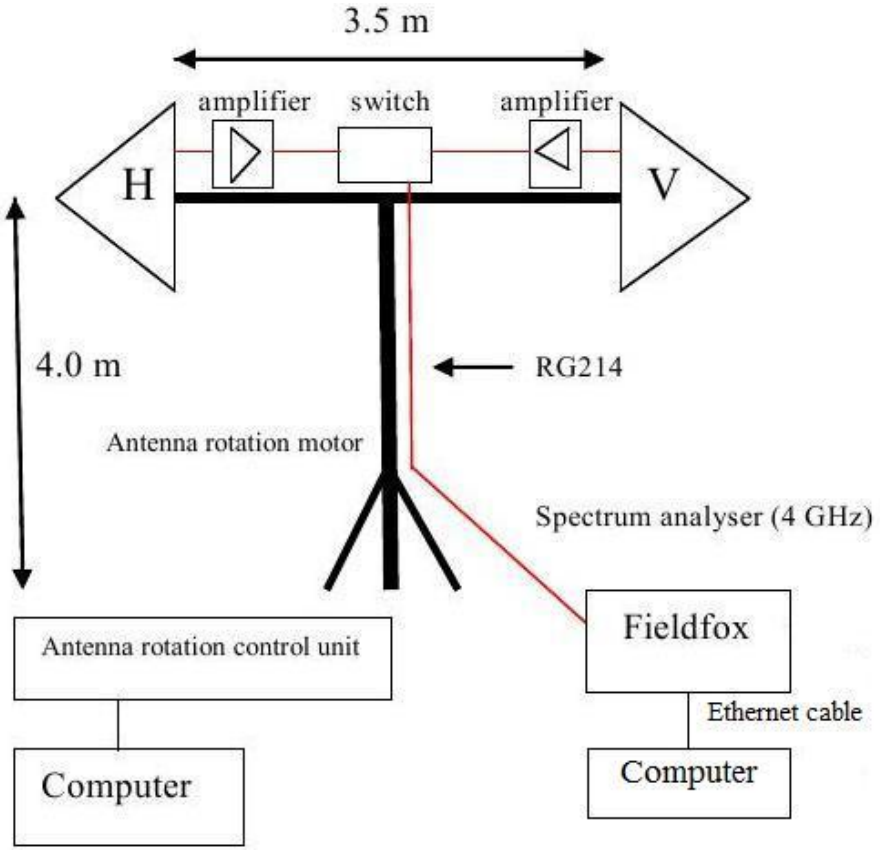

Figure 7.1: The rough schematics of the new RFI-monitoring system.

7.2 Other RFI monitoring improvements

It is essential to follow the development of the self-generated radio interference monthly or at least annually, depending on the acquired new electrical equipment. These measurements ought to be done in the control room or nearby, where the radiation is maximum. A suitable observation band is between 30-2600 MHz. A good reference for these internal RFI measurements is obtained, when the electricity in the MRO is turned OFF completely. It is also wise to measure the radiation of the new acquired equipment individually to determine their harmfulness. The RFI-monitoring system is also radiating interference in the employed observation band, which is likely to worsen with age, therefore the radiation should be measured from time to time. Some mitigation methods, like the Spectral Kurtosis (SK) introduced in Chapter 4.2.4 employ a hardware which produces a significant amount of radiation. The level of this radiation ought to be measured before utilizing the hardware.

Chapter 8

Results

The ambient radio frequency environment in the Metsähovi radio observatory (MRO) has evolved since the starting of the RFI monitoring in 1998. Numerous new radio applications are deteriorating the frequency spectrum each year. To gather more wideband information about the current state of the surrounding radio environment, a new RFI-monitoring system was built for the RFI measurements in this thesis. These measurements were done with horizontal and vertical polarization, between 350-2600 MHz in eight antenna positions. In these measurements, it was discovered that the strongest radio interference came from east, see Figure 8.1. Figure 8.2 shows the map of Helsinki Metropolitan area due east from Metsähovi. The nearest suburban areas are Lapinkylä (5 km), Espoo City Centrum (20 km), Kauniainen (23 km), Leppävaara (28 km) and Pasila (36 km) where the television tower is located. Approximately 42 km due east is the Malmi airport and a little further due north

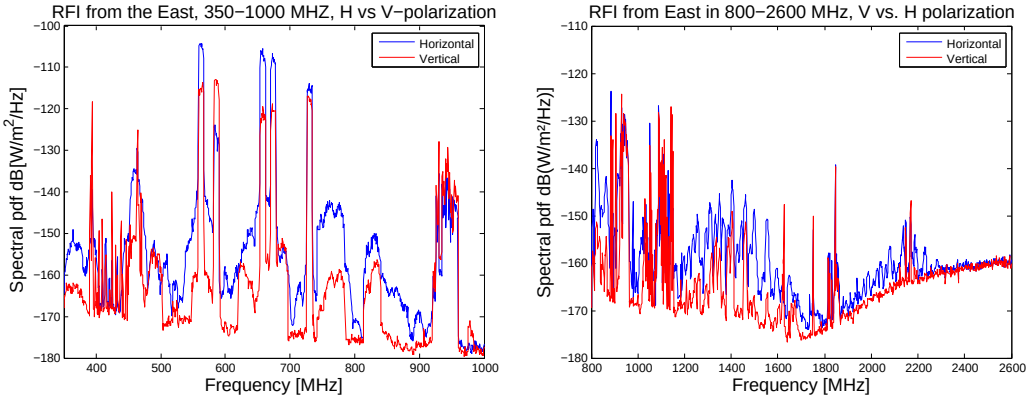

Figure 8.1: Radio interference from the east, with vertical and horizontal polarization between 350-2600 MHz.

the Helsinki-Vantaa airport. These active airports and the airplanes using them, are strong sources of radiation in their reserved radio bands. All the detected and identified interference sources in this particular band are listed in Table 8.1.

Table 8.1: Detected and identified RFIs in 350-2600 MHz band, from FICORA

RFI source	Frequency [MHz]	Detected spfd [dB(Wm^2/Hz)]	Description
VIRVE / TETRA	394	-120	
Wideband digital mobile communication network 450	462-466	-126	
Digital TV ch 32	562	-105	multiplex A
Digital TV ch 35	586	-130	
Digital TV ch 44	658	-108	multiplex B
Digital TV ch 46	674	-108	multiplex C
Digital TV ch 53	730	-115	multiplex E
Digital TV	740-790	-125	
Wideband digital mobile communication network 800	815-840	-135	
GSM-900	900	-120 -150	downlink 921-960, uplink 876-915
Aviation radio traffic DME	960-1164 962-1213	-118	
Aviation radio navigation Radars	1300-1350	-152	
Iridium	1618-1630	-147	
GSM-1800	1847 1751	-132 -151	downlink 1805-1880, uplink 1710-1784
IMT (3G)	2110-2170	-142	
Microwave ove	2400-2475	-140	

Using the astronomical radio receivers as RFI monitors, useful information can be harvested by studying the IF channel spectrum of the receiver with a spectrum analyser. The RFI tolerance of three radio receivers were tested, S-band, X-band and 22 GHz-VLBI, the results are presented in Figure 8.3. In these measurements, the radio telescope was set to sweep to horizon with low elevation ($e \sim 5°$), the IF spectrum was recorded from the spectrum analyser with a laptop in eight antenna positions.

Figure 8.2: Suburban areas due east from Metsähovi,(Google-maps).

In Figure 8.3 (top), is the S-band receiver IF spectrum recorded from east (left) and south-west (right). The strong interference on rising edge of the signal band is from the UMTS (3G-network) in 2170 MHz. The interference signal in the signal band (right) is from a radio amateur beacon in Inkoo circa 45 km away. This interference weakens rapidly when the elevation is increased. The 3G network interference doesn't have a strong elevation nor azimuth dependence, this interference is always present in the S-band measurements by leaking in through a side lobe of the antenna pattern. The sensitivity of the S-band receiver has weakened since the year 2009 with few dBm, which is approximately the same time when the 3G network was first utilized in urban areas. Unfortunately the old RFI monitor's frequency band was extended only in 2000 MHz, therefore there is no knowing when the 3G network started to affect the astronomical observations in the MRO. The effects of this interference ought to be studied more. The question is, are these 3G broadcasts able to saturate the amplification of the front end LNA and lead to the noticed sensitivity loss?

An X-band receiver measurement in Figure 8.3 (middle) showed no sign of interference. It's safe to say that X-band measurements are not corrupted by the presence of internal nor external RFIs. The third tested receiver was 22 GHz-VLBI, the results are shown in Figure 8.3 (bottom). On the left is the IF-spectrum of the receiver when the antenna was pointed toward east and on the right is the corresponding spectrum from the south. The IF channel showed extraordinary behaviour when the telescope is looking east with 5° elevation. The IF signal band is totally distorted. The nearby signal bands are reserved for Short Range Radar systems (SRR) 21.650-23.600 GHz and radio links 22.078 -23.600 according to FICORAs frequency

allocation. When the telescope was pointed toward south (right), the IF channel showed loads of small ripples in the spectrum, caused by an unknown interference source or sources. To identify these interference sources, more investigation ought to be done.

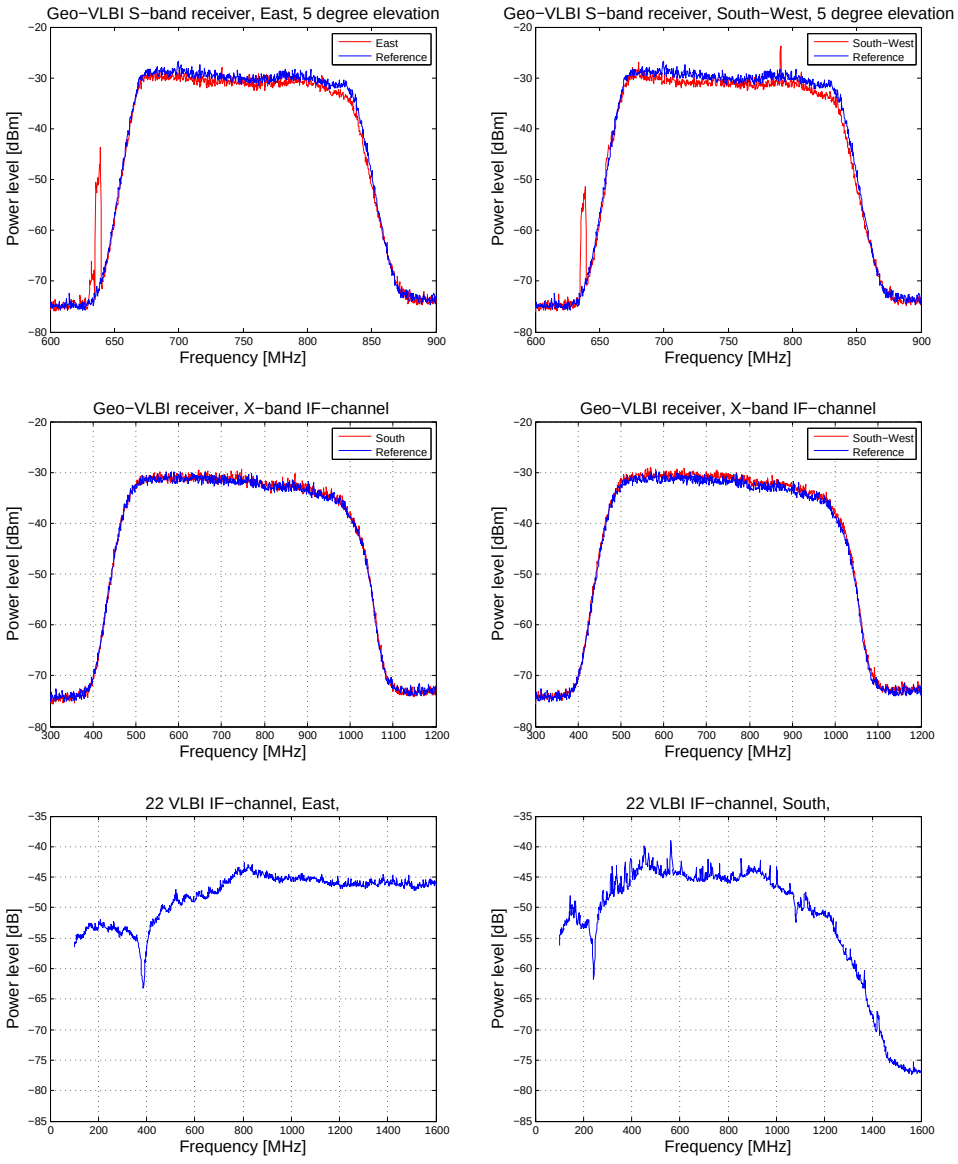

Figure 8.3: Astronomical radio receivers S-band(top), X-band (middle) and 22 GHz-VLBI (bottom) IF channel measured with spectrum analyser in different antenna positions.

Radio observatories are themselves a significant source of radio interference. The amount of internal radiation was measured between 30-2600 MHz band with a log-periodic antenna and a spectrum analyser. The results are presented in Figure 8.4. The antenna was placed under the radio telescope circa 10 meters away from the control room (left) and inside the control room (right). These plots show significant amounts of narrow band internal RFI under 1 GHz. The use of mobile phones (GSM-900) is also visible in these measurements, although the use of radio transmitters of all kind is prohibited in the observatory grounds. The wideband interference between 2410-2470 MHz is the microwave oven, which is a most significant source of internal radiation. Some of the internal RFI sources were also measured individually, such as, microwave oven, mobile phone, hydrogen maser along with a few other scientific instruments. The results of these measurements are found in Figure 8.5.

The amount of internal radiation, can be reduced by prohibiting the use of radio transmitters and placing the mandatory scientific instruments inside a Faraday cage if possible. Against the external RFIs, observatories can use several pro- and re-active mitigation methods introduced in Chapter 4. One of the most promising new mitigation methods in radio astronomy is called Spectral Kurtosis (SK). It is proven to be so effective in removing the RFIs from the astronomical data, that it might become a standard for next generation radio telescopes.

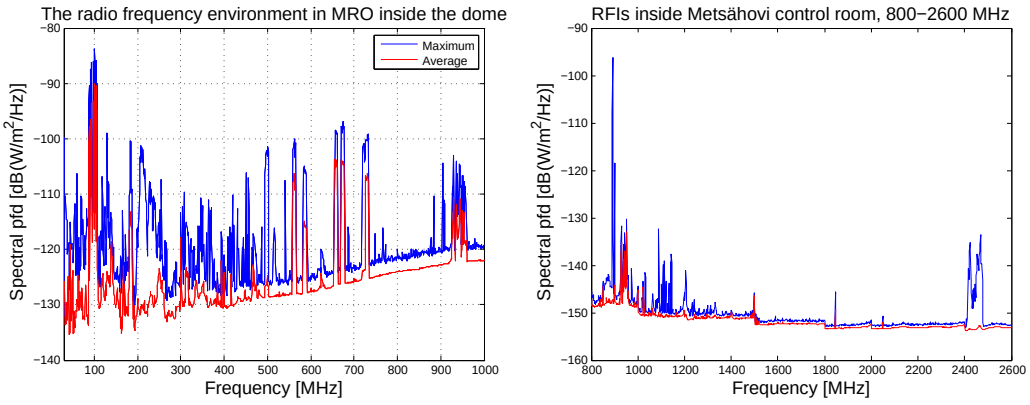

Figure 8.4: Internal radio frequency in the MRO, between 30-2600 MHz.

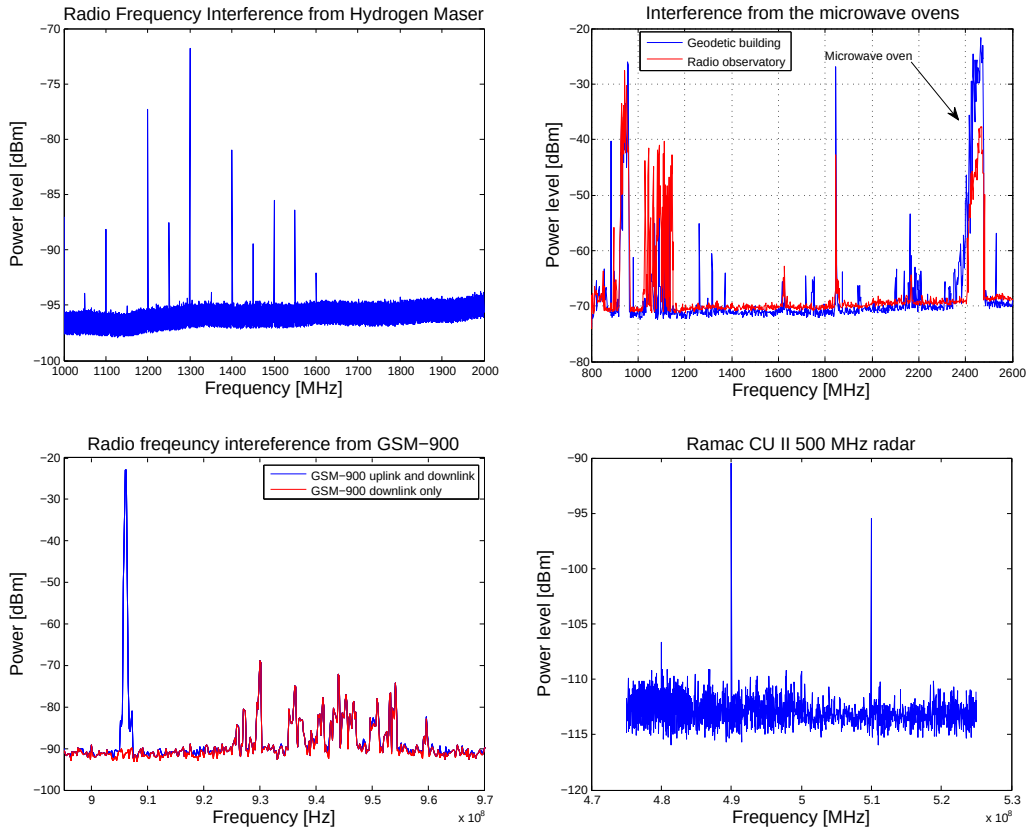

Figure 8.5: Individual internal RFI sources: hydrogen maser (top/left), microwave oven (top/right), mobile phone (bottom/left) and Ground Pentrating Radar GPR (bottom/right).

Chapter 9

Conclusions

Radio frequency interference is an ever increasing problem in radio astronomical measurements. All kind of radio broadcasts and new radio applications are deteriorating the radio frequency spectrum at the observatory site each year. Consequently radio observatories are also generating remarkable amounts of radiation themselves, which might cause distortion to the astronomical data.

This thesis discusses, the impact of the radio interference in observation, interference monitoring techniques and the potential mitigation methods to minimize the effects of the radio interference. The radio frequency environment has been monitored constantly in the Metsähovi Radio Observatory for over a decade. The observed frequency band covers only the IF spectrum of the astronomical radio receivers. This thesis provides, wideband measurements with two different polarizations to determine the current state of the surrounding radio frequency environment at the observatory site. Furthermore, a great number of measurements were also done to determine the amount of internal radiation generated by the electrical equipment inside the facility. Some of these internal interference sources were identified and measured individually to determine their harmfulness in radio astronomical observation. Multiple high frequency radio receivers employed in astronomical observation were also used as a radio frequency monitor, to investigate the abundance of the interference in the signal band. The significance of the radio interference in radio astronomy should not be taken lightly. It is crucial to continue the constant monitoring of the external and internal radio frequency environment in the future. To ensure the reliability of the astronomical measurements, interference measurements ought to cover the IF and the RF spectrum of the astronomical radio receivers.

REFERENCES

[1] Southworth, G. C., *Early history of radio astronomy,* The Scientific Monthly, 1965.

[2] Räisänen, A. and Lehto A., *Radiotekniikan perusteet,* Otatieto, 2001.

[3] Mallat, J. A., *Sensitivity aspects of radio telescope receivers for astronomy,* Helsinki University of Technoly 1995.

[4] Nelson, R. A., *Antennas: Interface with space,* http://www.aticourses.com/antennas_tutorial.htm.

[5] Steinberg, J. L., *Radio Astronomy,* McGraw-Hill Electronic science series, 1963.

[6] Tiuri, M. E., *Radio Astronomy receivers,* Antennas and propagation, IEEE transactions on, vol. 12, pp. 930-938, 1964.

[7] The Committee on Radio Astronomy Frequencies (CRAF), *Radio frequencies of the astrophysically most important spectral lines,* http://www.craf.eu/iaulist.htm, 2003.

[8] Lopez-Perez, J. A., *Detected Interferences at S-band from the 40-m Radiotelescope Servo Systems,* Observatorio de Yebes, Instituto Geografico Nacional, Spain, VLBI 2010/FRFF2009.

[9] Millenaar, R. P. and Stiepel H. J., *On self-generated RFI at Radio Astronomy Sites,* Committee on Radio Astronomy frequencies, CRAF-04-1 , 2003.

[10] Crane, P. C. and Hillebrand L., *Estimating harmful levels of radio-frequency radiation,* Light Pollution, Radio Interference, and Space Debris, ASP Conference Series, vol. 17, 2003.

[11] Tuccari, G., *Interference at a VLBI Station: Analysis and Mitigation,* Istituto di Radioastronomia -INAF, 2009.

[12] RECOMMENDATION ITU-R RA.769-2, *Protection criteria used for radio astronomical measurements,* 2003.

[13] ASTRON Netherlands, CSIRO Australian Telescope National Facility, Nation Research Foundation South Africa, SKA Program Development Office and The University of Manchester United Kingdom, *Agreement on Radio Frequency Interference (RFI) monitoring 2008-2011,* 2008.

[14] Grypstra, K. and Keller, R., *The frequency coverage and RFI observations at Effelsberg,* Max-Planck-Institut für Radioastronomie, 2009.

[15] Fischer, J. R. and Beaudet, C., *Sensitivity comparison of RFI monitor station and GBT L-band receiver,* Electronics Division Technical Note, no. 209, 2007.

[16] Beaudet, C., *The Greenbank interference protection group: Policies for RFI management,* 2007.

[17] Rogers, E. E., *RFI shielding and mitigation techniques for a sensitive search for the 327 MHz line of Deuterium,* M.I.T Haystack Observatory, 2007.

[18] Ravier, P., *Robust mean estimation for real-time blanking in radio astronomy,* Laboratory of Electronics, Signals, Images, Polytech Orléans- University of Orleans, 2009.

[19] Gilloire, A. and Sizun, H., *RFI mitigation of GNSS signals for radio astronomy: problems and current techniques,* Ann. Telecommun, vol. 64, no. 9-10, pp. 625-638 2009.

[20] Kesteven, M., *The current status of RFI mitigation in radio astronomy,* Australia Telescope National Facility. CSIRO, 2009.

[21] Fridman, P. A. and Baan, W. A., *RFI mitigation methods in radio astronomy,* Astronomy & Astrophysics, ASTRON, Netherlands Foundation for Research in Astronomy, and Westerbork Observatory, vol. 378, no. 1, pp. 327-344, 2001.

[22] Raza, J. and Boonstra, A-J., *Spatial filtering of RF interference in radio astronomy,* IEEE Signal Processing Letters, vol. 9, no. 2, pp. 64-67, 2002.

[23] REPORT ITU-R RA.2126, *Techniques for mitigation of radio interference in radio astronomy,* 2007.

[24] Ruf, C., *Detection and mitigation of radio frequency interference using a digital Kurtosis spectrometer/detector,* Space Physics Research Laboratory, of Atmospheric, Oceanic and Space Science, University of Michigan.

[25] Gary, D. E. and Nita, G. M., *A wideband spectrometer with RFI detection,* Publication of Astronomical Society of the Pacific, 2010.

[26] Kirves, P. and Kallunki, J., *RFI in Metsahovi Radio Observatory - measurements and effects,*, Aalto university Metsähovi Radio Observatory, Proceeding of Science, RFI mitigation workshop - RFI2010, 2010.

[27] Wade, P., *Parabolic dish antennas,* N1BWT, ch 4, 1994.

[28] McLean, J. and Sutton, R., *Interpreting antenna performance parameters for EMC applications: Part 3 Antenna factor,* TDK RF Solutions Inc, Literature Requests, Brochures Articles, Interpreting Antenna Performance Parameters for EMC Applications, part 3, pp. 18-26.

[29] Lehto, A. and Räisanen, A., *Mikroaaltomittaustekniikka,* Otatieto Oy, 2001.

[30] Fortesque, P. and Stark, J., *Spacecraft systems engineering,* Wiley, Third Edition, 2004.

Appendix A

Radio frequencies in radio astronomy

Frequency band	Bandwidth	Applications	Protection
25.550-25.670 MHz	120 kHz		
1400-1427 MHz	27 MHz		**
1660-1660.500 MHz	500 kHz		
1660.500-1668.400 MHz	7.900 MHz		
1668.400-1670.000 MHz	1.600 MHz		
2690-2700 MHz	10 MHz		
4990-5000 MHz	10 MHz		
10.680-10.700 GHz	0.020 GHz		
15.350-15.400 GHz	0.050 GHz	VLBI	
22,210-22,500 GHz	0,290 GHz	Used in Metsahovi, Sun observation ,VLBI, Water vapor emissio, Continuum, Spectral line	
23.600-24.000 GHz	0.400 GHz	Water vapor emission line	**
31.300-31.500 GHz	0.200 GHz		**
31.500-31.800 GHz	0.300 GHz		
36-37 GHz	1 GHz	Continuum, Sun	
42.500-43.500 GHz	1 GHz	Continuum, Sun, VLBI	
48.940-49.040 GHz height76-77.750 GHz	0,100 GHz 1,500 GHz		
77.500-78.000 GHz	0,500 GHz		

Frequency band	Bandwidth	Applications	Protection
78-79 GHz	1 GHz		
79-81 GHz	2 GHz		
81-84 GHz	3 GHz		
84-86 GHz	2 GHz		
86-92 GHz	6 GHz	Continuum, Spectral line, Sun observation, VLBI	**
92-94 GHz	2 GHz	Spectral line	
94,000-94.100 GHz	100 MHz		
94.100-95.000 GHz	900 MHz		
95-100 GHz	5 GHz	Continuum, Spectral line	
100-102 GHz	2 GHz	Continuum, Spectral line, Sun observation, VLBI	**
102-105 GHz	3 GHz	Continuum, Spectral line, Sun observation, VLBI	
105-109.500 GHz	4.500 GHz	Continuum, Spectral line, Sun observation, VLBI	
109.500-111.800 GHz	2.300 GHz	Continuum, Spectral line, Sun observation, VLBI	**
111.800-114.250 GHz	2,450 GHz	Continuum, Spectral line, Sun observation, VLBI	**
114.250-116.000 GHz	1,750 GHz	Continuum, Spectral line, Sun observation, VLBI	**
130-134 GHz	4 GHz		
34-136 GHz	2 GHz		
136-141 GHz	5 GHz		
148.500-151.500 GHz	3 GHz		**
151.500-155.500 GHz	4 GHz		
155.500-158.500 GHz	3 GHz		
164-167 GHz	3 GHz		**
182-185 GHz	3 GHz	H20 spectral line	
200-202 GHz	2 GHz		**
202-209 GHz	7 GHz		**

Frequency band	Bandwidth	Applications	Protection
209-217 GHz	8 GHz		
217-226 GHz	9 GHz		
226.000-231.500 GHz	5.500 GHz		**
241-248 GHz	7 GHz		
248-250 GHz	2 GHz		
250-252 GHz	2 GHz		**
252-265 GHz	13 GHz		
265-275 GHz	10 GHz		

* = frequency bands where all the other broadcast are prohibited